Master of Science Thesis in Electrical Engineering
Department of Electrical Engineering, Linköping University, 2020

Strategies for road profile in adaptive suspension control

Fredrik Skoglund

Master of Science Thesis in Electrical Engineering

Strategies for road profile in adaptive suspension control:

Fredrik Skoglund

LiTH-ISY-EX--20/5317--SE

Supervisor: **Victor Fors**
ISY, Linköpings universitet
Anton Albinsson
Volvo Cars

Examiner: **Jan Åslund**
ISY, Linköpings universitet

Division of Vehicular Systems
Department of Electrical Engineering
Linköping University
SE-581 83 Linköping, Sweden

Abstract

Semi-active suspension systems has become an increasingly popular alternative to the passive suspensions in recent time. By varying the spring stiffness and damping coefficient in the system, different characteristics can be achieved depending on driver preferability and road disturbances. The difference in damping coefficient will however lead to a trade-off between comfort and road holding, which means that in order to improve one of the areas, performance in the other will need to be reduced. This trade-off will also be different depending on the underlying road disturbances.

This thesis is conducted on behalf of Volvo Cars, who are looking for a strategy in order to analyze the trade-off for different ISO classified roads which has been done through a literature study, theoretical analysis and comparison of control methods for different roads. A skyhook based controller was built with added modifications in order to reduce the jerk in the vehicle. Tests with the controller were carried out on a quarter car model as well as a full car model in IPG Carmaker. The simulations with the quarter car model showed that the controller improved the peak jerk values as well as the comfort, compared to both skyhook control and passive suspension.

The full car simulations consisted of test runs on four roads, all with different road profiles and frequency content. For each road, tests were conducted with two different damper control methods as well as with a varying spring stiffness. The tested damper control methods were force gain control, which modulates the force request from the skyhook controller, as well as rate limitation control, which modulates the rate at which current is applied to the damper. The results showed that the trade-off between road holding and comfort appeared differently when the road profile changed. All results were compared to Janeway's comfort criterion in order to validate the comfort of the vehicle. The outcome of the thesis was a strategy that involved various tuning for the semi-active damper and air suspension depending on the primary and secondary ride nature of the road. More specifically, a stiff damping is preferred during general primary ride conditions and a soft damping is preferred during general secondary ride conditions. For cases when the low frequency disturbances are small, the trade-off will be small and comfort can be improved with little to no cost of road holding. When the high frequency disturbances increase in amplitude, the damper should be tuned depending on preferability. For improved road holding ability, a stiff damping is preferred and for improved comfort, a soft damping is preferred. A soft spring will, for most cases, be preferred in terms of both road holding and comfort.

Acknowledgments

I would like to begin by expressing my most sincere gratitude towards all of the employees and fellow thesis workers at Volvo Cars who has shown great support and encouragement. A special thank you to Anton Albinsson, who has provided excellent knowledge and guidance over the course of the semester.

I would also like to thank my supervisor at Linköping University, Victor Fors, who has provided continuous guidance and invaluable discussions.

Gothenburg, May 2020
Fredrik Skoglund

Contents

Figures

Tables

1 Introduction

This chapter consists of a problem description and problem formulation along with a literature review of related research and thesis outline.

1.1 Description

Ride comfort is an important aspect in cars. To minimize the acceleration of the vehicle body, and thus increasing comfort, caused by vibrations from the road a suspension is used. While ride comfort is important for the overall experience in a car it is also an important aspect in terms of safety since vibrations will cause drive fatigue, more so after long exposure. The suspension is also responsible for the road handling ability of the vehicle. These two aspects are hard to achieve simultaneously and have to be weighed against each other.

In recent times, semi-active and active suspension systems have become options to the regular passive suspension system. These systems allow for the driver to adjust the settings with regards to the wanted driving experience. While semi-active systems only allow for damping in the direction opposite to the suspension velocity, active systems are able to provide forces both up and down, not dependent on the current movement of the suspension system. Since active systems require expensive actuators, semi-active systems are more common as they are able to provide similiar ride comfort.

The amount of damping affects both the ride comfort along with the grip between tire and road. While a high damping will lead to good ride comfort at low frequencies, the body accelerations will increase at high frequencies.

1.2 Problem formulation and objective

Semi-active and active suspension systems are usually offered as an option to improve ride comfort. This is achieved by controlling the vertical suspension forces by controlling the damping coefficient and consequently the body and wheel motion. However, the level of damping also affects the grip between the tire and the road. The semi-active dampers have a limited bandwidth and high frequency disturbances can therefore not actively be attenuated. Higher damping leads to a lower body acceleration at low frequencies but higher body accelerations at high frequencies. Hence, if the body motion is controlled by high damping on a road with high frequency disturbances, the vibration level is compromised. Another system that is gaining popularity in the industry is adjustable suspension stiffness. High suspension stiffness increases the body acceleration for both low and high frequencies.

The fact that high damping is required for improved road handling and low damping is required for improved ride comfort at high frequencies presents a trade-off. The trade-off between body control and vibration levels always has to be considered for both semi-active dampers and for adjustable spring stiffness. However, the trade-off will be different for different roads. For roads with high amplitude at high frequencies, the amount of body control must be compromised in order to maintain an acceptable vibration level. With information about the amplitude of the road disturbances for different frequencies, the tuning of the damper controller and adjustable stiffness can be adjusted to be the current road surface and thus improve the overall ride experience on all roads.

The thesis is written for the Volvo Cars, which is a company that has been developing and manufacturing automobile vehicles since 1927. Today the company is known for its luxurious vehicles and cutting edge technology.

The objective of this thesis is to find a strategy to optimize the trade-off between road handling and ride comfort on different classifications of road. The road classifications will be defined between A through F and will represent a different amount of road roughness, where A is the least rough road. Tests will be carried out in simulations in Simulink and IPG Carmaker.

The following questions will be answered in this thesis:

i. What strategy can be defined to weigh the damping and stiffness suspension parameters in order to improve handling and comfort for different road profile classifications?

ii. What performance criteria in terms of limits over different frequencies can be used to define good ride comfort and road handling?

iii. What benchmarks for suspension systems can be used that are representative for different degrees of model complexity and real-world driving?

1.3 Related research

1.3.1 Semi-active suspension control

A lot of research in the active and semi-active suspension control area has been carried out since Citroën first introduced the hydropneumatic suspension in 1954.

Liu et al. [11] compared five different control strategies based on skyhook control, balance control and adaptive control. Ślaski et al. [9] compared a traditional on-off skyhook controller with fuzzy logic applied to the skyhook controller which resulted in an improved trade-off between body and wheel displacement as well as improved opportunities for control strategy. Sammier et al. [13] compared an H_∞ control with skyhook control. The results showed that an increased ride comfort could be achieved with the H_∞ approach. Skyhook control was however preferred in terms of simplicity in modeling and ability to control the trade-off between ride comfort and road handling.

The dampers in a semi-active suspension system has a limited working region. When the working region is entered or exited the control force will be changed abruptly, this will create a jerking motion which in turn will cause decreased ride comfort. Stamatov et al. [18] proposed a time based modulation to solve this issue. It resulted in improved characteristics compared to a similar level-based method. Lindgärde [10] implemented a model-based estimator including a Kalman filter to estimate the vertical velocity and the relative damper velocity.

Ghasemalizadeh et al. [3] compared two comfort-based control methods, acceleration driven damping (ADD) and power driven damping (PDD), with an H_∞ robust control method. The results showed that H_∞ robust control gave both a better ride comfort as well as an improved road handling explained by a decrease in center of gravity acceleration. Gustafsson et al. [5] developed an artificial neural network, trained with reinforcement learning, as a method to control the suspension. The results were promising considering its low computational requirements but the controller couldn't perform on the same level as a regular model predictive controller (MPC). Darus et al. [1] implemented a linear quadratic regulator (LQR) on a full car model using active suspension. The results showed limitations in performance under rough conditions.

Madhusudhana [12] developed a method to classify a road according to ISO 8608 with the use of H_∞ robust control and power spectral density (PSD) analysis.

1.3.2 Ride comfort

Ride comfort is an abstract area since comfort can be defined differently for every human. Janeway [7] suggested that an amplitude limit should be introduced for three different frequency areas. More specifically, the peak value of jerk should be limited to $12.6ms^{-3}$ in the frequency range 1-6Hz, the peak value of acceleration should be limited between 6-20Hz to $0.33ms^{-2}$ and in the 20-30Hz frequency range the peak value of velocity should be limited to $2.7mms^{-1}$. ISO 2631 appears

to be the most common standard that is not only used in the automotive industry, but for vibrations in general [4]. This method uses root mean square (RMS) to quantify discomfort, proficiency and preservation in the 1-80Hz frequency range.

1.4 Outline

This thesis consists of the following chapters:

- **Introduction:** A description of the project is presented along with a problem formulation, thesis objective and related research.
- **Theory:** In this chapter a theoretic background regarding suspension systems, control and analysis methods is presented.
- **Controller implementation:** In this chapter a damper controller is modeled.
- **Quarter car model simulation:** In this chapter tests are carried out on a quarter car model with the modeled controller.
- **Full car model simulation:** Simulations are made on a full car model in IPG carmaker for various road profiles and controller parameters and the results are compared.
- **Discussion and conclusion:** In this chapter a discussion is made with respect to the achieved results and a conclusion is presented. The research questions from section 1.2 are answered and a future scope is presented.

2
Theory

This chapter consists of a theoretic background with regards to vehicle dynamics, vibrations and analysis methods.

2.1 Vehicle theory

The movements in a vehicle are caused by a combination of rotational and translational movements.

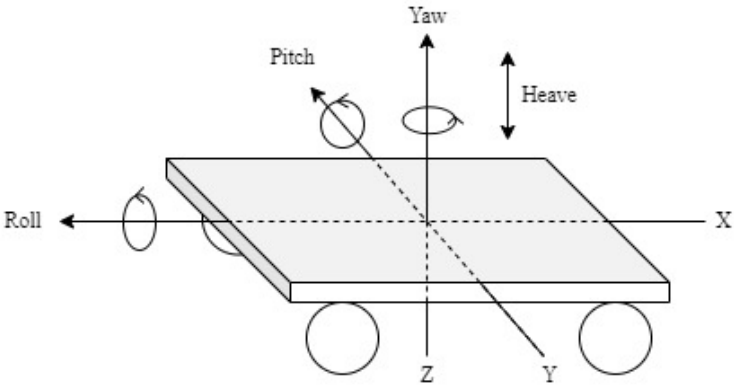

Figure 2.1: *The dynamic motions of a vehicle*

The rotational movement around the lateral axis (Y-axis) is called **pitch**. Pitch is noticed primarily in acceleration, deceleration and breaking but is also caused

by road disturbances. Pitch movements are hard to reduce but can be attenuated with proper damper control.

Roll is the rotational movement around the longitudinal axis (X-axis). The roll movements are primarily noticed during cornering, but are also felt on roads where the road profile highly differs from the right to left side of the vehicle. These movements are reduced with the use of an anti-roll bar, explained in section 2.3.3, as well as with the use of damper control.

Yaw movements are rotational movements around the vertical axis of the vehicle (Z-axis). Yaw movements happen mainly as a response to steering input, but is also caused by winds affecting the vehicle. These movements are primarily reduced by adjusting the aero dynamics and suspension settings, which isn't possible during operation.

Translational movements along the vertical axis is called **heave**, sometimes referred to as **bounce**, and is mainly caused by road unevenness and can be reduced with damper control.

While only the primary causes of the rotational and translational movements has been explained above it should be mentioned that all movements are a combination of different forces acting on the vehicle. Not showing in figure 2.1 are the translational movements along the lateral and longitudinal axes. The movement along the longitudinal axis is called **sway**, but is more commonly referred to as acceleration and deceleration. The lateral movement is called **surge** and happens as a response to the forces caused during cornering. This movement is reduced through a good suspension setup and good selection of tires.

2.2 Vibrations

The body and suspension will need to adapt to vibrations no matter what the drive conditions are like. The frequency and amplitude of these vibrations will vary over different roads.

2.2.1 Ride comfort

Ride comfort can be divided into two different areas, primary- and secondary ride. Primary ride is defined by disturbances with low frequency (around 0-4Hz) and high amplitude. This is more easily defined as movement over road variations visible to the human eye. Secondary ride refers to disturbances not visible to the human eye (around 4-25Hz) in the low amplitude - high frequency range. In general, during lower speed the primary ride is improved with a worsened secondary ride, and at high speed the primary ride is more noticable with an improved secondary ride. Humans are most sensitive to excitations in the 4-8Hz range [2].

Since comfort and discomfort are highly subjective areas of measure it is difficult to define an optimum value with which both areas will be seen as ideal. Various

methods can be used to analyze ride comfort in vehicles but in this report, the ride comfort will be analyzed through frequency analysis of the body acceleration as well as the peak values of jerk.

2.2.2 Road holding

The road holding of a vehicle can be defined as the tires ability to stay in contact with the road when driving on a road with vertical irregularities with a certain speed [2].

The road holding ability of a vehicle is commonly analyzed through the frequency response of the tire deflection. By varying the damping coefficient and spring stiffness, the transmissibility of disturbances in the low and high frequency domain will change, further explained in section 2.3.

2.2.3 Power spectral density analysis

The power spectral density (PSD) shows the power of the signal over different frequencies. The avarage power, P, for a signal x(t) is described by:

$$P = \lim_{t_f \to \infty} \frac{1}{t_f} \int_0^{t_f} |x(t)|^2 dt \tag{2.1}$$

The signal can then be described in the frequency domain through a fourier transform as follows:

$$\hat{x}(\omega) = \frac{1}{\sqrt{t_f}} \int_0^{t_f} x(t) e^{-i\omega t} dt \tag{2.2}$$

Where $\hat{x}(\omega)$ is the amplitude spectral density. Thus, the power spectral density, $S_{xx}(\omega)$, can be defined as:

$$S_{xx}(\omega) = \lim_{t_f \to \infty} \mathbf{E}\left[|\hat{x}(\omega)|^2\right] \tag{2.3}$$

Where **E** describes the expected value such as:

$$\mathbf{E}\left[|\hat{x}(\omega)|^2\right] = \lim_{t_f \to \infty} \int_0^{t_f} \int_0^{t_f} \mathbf{E}\left[x^*(t)x(t')\right] e^{-i\omega(t-t')} dt dt' \tag{2.4}$$

By assuming a stationary random process, the signal $S_{xx}(\omega)$ and autocorrelation function of the signal can be seen as Fourier transform pairs. The autocorrelation function is given by:

$$R_{xx}(\tau) = X(t)X(t-\tau)^* \tag{2.5}$$

Assuming $R_{xx}(\tau)$ is integrable, the PSD can then be described by the function:

$$S_{xx}(\omega) = \int_{-\infty}^{\infty} R_{xx}(\tau) e^{-i\omega\tau} d\tau = \hat{R}_{xx}(\omega) \tag{2.6}$$

The vertical road profile can typically be described as a combination of sinusoidal waves with different frequencies and amplitude, which will cause displacements in the vehicle body and suspension. PSD analysis can thus be used to analyze the impact of the vibrations that the road has on the vehicle and suspension. The amplitude of these vibrations will have different impact on the vehicle depending on the frequency. Vibrations close to the wheel hop frequency, explained further in section 2.3, at around 10Hz will be amplified as well as vibrations close to the body resonance frequency, at about 1-2Hz.

Ride comfort and road holding can be analyzed through PSD analysis of body acceleration and tire deflection, explained in 2.2.1 and 2.2.2.

2.2.4 Root mean square

Root mean square (RMS) is a useful tool for analyzing vibrations over frequency ranges. The RMS value of a signal over a certain freqency range $\omega_0 \rightarrow \omega_1$ can be obtained as:

$$RMS(x(t)) = \sqrt{\int_{\omega_0}^{\omega_1} S_{xx}(\omega) d\omega} \tag{2.7}$$

Where x(t) is the signal in the time domain and $S_{xx}(\omega)$ is the PSD of the signal in the frequency domain. The RMS value of a signal can also be described as the area under the curve of the PSD signal.

2.2.5 Performance index

A performance index can be used to visualize the trade-off between comfort and road holding. One performance index, developed by Savaresi et al. [17], is as follows:

$$\mathscr{C}(X, \underline{f}, \overline{f}) = \int_{\underline{f}}^{\overline{f}} |X(f)|^2 df \tag{2.8}$$

Where X(f) is the signal of interest in the frequency domain. The parameters $\underline{f}$ and $\overline{f}$ are the lower and upper limits in the frequency range of interest.

The comfort criterion is based on body acceleration and is studied in the range of 4 to 20Hz, as this is the area for which humans are most sensitive, further explained in section 2.2.1. Road holding is studied for the tire deflection over the frequency range 0.5 to 30Hz. Since the bandwidth of the damper is limited,

signals above 30Hz and below 0.5Hz won't be attenuated which thus makes analysis of frequencies outside this range unnecessary. The comfort criteria, J_c, and road-holding criteria, J_{rh}, can thus be defined as:

$$\tilde{J}_c = \tilde{J}_{\ddot{z}_s} = \frac{\mathscr{C}(\tilde{F}_{\ddot{z}_s}, 4, 20)}{\mathscr{C}(\tilde{F}^{nom}_{\ddot{z}_s}, 4, 20)} \tag{2.9}$$

$$\tilde{J}_{rh} = \tilde{J}_{z_{def_t}} = \frac{\mathscr{C}(\tilde{F}_{z_{def_t}}, 0.5, 30)}{\mathscr{C}(\tilde{F}^{nom}_{z_{def_t}}, 0.5, 30)} \tag{2.10}$$

Where $\tilde{F}_{\ddot{z}_s}$ and $\tilde{F}_{z_{def_t}}$ are the variance gains of the comfort signal $\ddot{z}_s$ and road holding signal z_{def_t}. $\tilde{F}^{nom}_{\ddot{z}_s}$ and $\tilde{F}^{nom}_{z_{def_t}}$ are thus the nominal variance gains.

The performance indices can be used in order to compare different control methods. To compare different methods a reference needs to be set for the nominal parameters and can be evaluated as follows:

- If $\tilde{J}_c < 1$, the analyzed suspension is more comfortable than the reference suspension.
- If $\tilde{J}_c > 1$, the analyzed suspension is less comfortable than the reference suspension.
- If $\tilde{J}_{rh} < 1$, the analyzed suspension has better road holding than the reference suspension.
- If $\tilde{J}_{rh} > 1$, the analyzed suspension has worse road holding than the reference suspension.

2.3 Suspension system

The suspension system is what connects the vehicle body to the road. The design of the suspension system will have an impact on ride comfort, suspension loads as well as road grip. Road grip is a combination of vertical forces caused by road disturbances, camber angle as well as user inputs such as steering angle and wheel forces from propulsion and breaking [17].

The suspension is different in every car but does in general consist of the same basic parts: linkages, dampers, tires and springs.

2.3.1 Linkages

The linkages in a suspension system can be explained as the connection of lateral and longitudinal forces from the wheel and the body. The function of the linkages is to constrain the movement of the suspension in extreme cases. Each pivot point in the suspension has bushings, which has their individual stiffness and damping. The stiffness and damping of the bushings are however much larger than in the springs and dampers.

2.3.2 Dampers

The function of the dampers is to dissipate the energy of the oscillations caused by the road. The method used to dissipate the energy can either be passive, semi-active or active. These methods are presented below.

Passive suspension

A passive suspension utilizes a spring and damper system with characteristics being set during the manufacturing of the car. The main benefits of this method is its good road handling abilities during normal driving conditions as well as its cheap price. Due to the characteristics of the spring and damper being set for the most used driving conditions i.e. asphalt roads, the road handling ability and comfort is reduced when these conditions change to e.g. bumpy roads.

Semi-active suspension

The semi-active suspension, or adaptive suspension as it's sometimes called, consists of a constant- or variable spring as well as a variable damper [17]. These systems are the most commonly used in modern vehicles due to its relatively cheap price as well as its good road handling abilities and increased comfort. Road holding ability can be analyzed through the frequency respone of the unsprung mass, explained in section 2.2.3.

When driving close to the wheel hop frequency, which is the natural frequency of the unsprung mass and is further explained in section 4.1, a stiff suspension would be preferred while a soft suspension would be preferred in lower frequencies. Along these lines, a high damping would be preferred around the natural frequency of the sprung mass, explained in section 4.1, in order to reduce the amplitude of the vibrations while a low damping would be preferred during high frequency disturbances. This does however present a problem since a low damping during high frequencies cause a decrease in road handling. These adaptions to the suspension parameters during the ride would not be possible with a passive suspension which is the main reason for the popularity of the semi-active suspension.

In figure 2.2, the impact that varying damping values has on comfort and road holding can be seen.

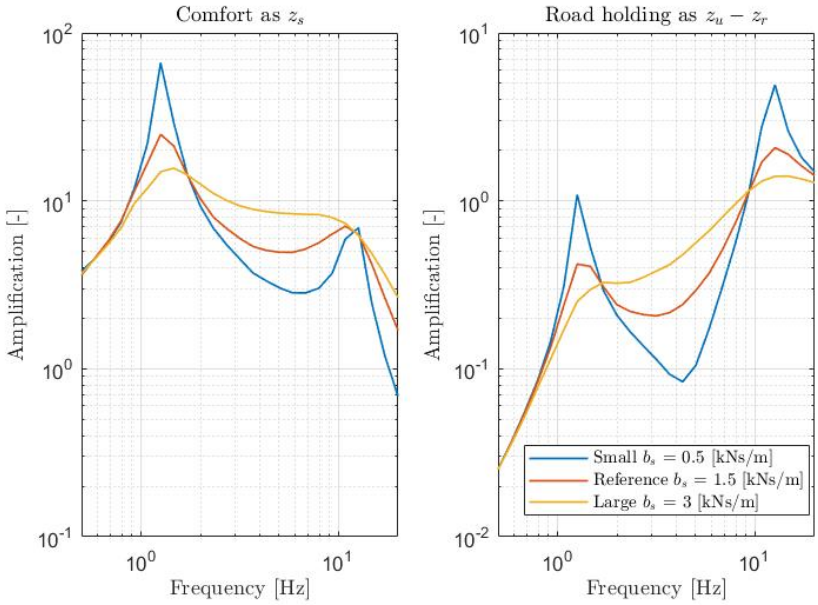

Figure 2.2: *Transfer function from road to vertical displacement (z_s) and road holding ($z_u - z_r$) for varying damping coefficients.*

In terms of comfort it can be seen that by lowering the damping coefficient is the transmissibility for low frequencies increased, while medium and high frequencies show an improvement. For road holding it can be seen that the transmissibility is increased for both frequencies around body resonance frequency as well as around the wheel hop frequency, while it is decreased for the medium frequencies when the damping coefficient is lowered.

In semi-active suspenson systems the most common shock absorber used is the hydraulic damper [17]. Applying a current to a solenoid valve placed at the damper makes it possible to adjust the flow of the hydralic fluid in the damper, which in turn makes it possible to adjust the amount of damping applied.

Another recent method of semi-active damping is the magnetorheological damper (MR damper) [17]. The MR damper uses a magnetorheological fluid, which has the ability to change its viscosity when subjected to a magnetic field, in order to change the stiffness of the damper. When the magnetic field is applied, e.g. through a electromagnet, the magnetic particles in the fluid changes from a random distribution to aligning themselves with respect to the direction of the magnetic flux, which in turn increases the fluid viscosity.

Active suspension

In recent times, the active suspension has become increasingly evaluated. By either replacing the spring and damper with an actuator or adding it in parallel,

the wheels can then be attenuated individually with the help of different sensors on the vehicle body and suspension. In semi-active suspension systems the damping force can only be applied in the opposite direction of the suspension deflection velocity, which is not the case for active suspensions. The active suspension system can provide a force in all directions, shown in 2.3, which gives more opportunities to improve ride comfort and road holding. While both road handling and comfort can be increased with this type of suspension, its expensive price tag is what causes semi-active suspensions to be more popular.

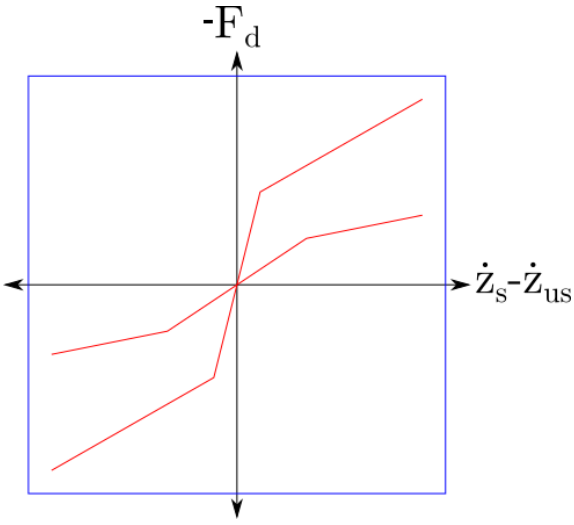

Figure 2.3: *Damper working space for active suspension (inside the blue square), not dependent on the direction of the damper velocity, and for semi-active suspension (between the red lines), dependent on the direction of the damper velocity.*

2.3.3 Springs

The function of springs in a suspension system is to carry the static load of the car body and allow for movements around its steady state during rebound and compression [17].

Anti-roll bar

The anti-roll bar (ARB) is a common part in suspension systems and is used to reduce body roll [17]. This is achieved by placing the ARB in between the wheels, also known as the springs axle, and thus making them dependent of each other.

Passive spring

The passive spring deliveres a force as a reaction of movements in the ground, as shown by:

$$F = kx \tag{2.11}$$

Where F is the spring force, k is the spring stiffness and x is the displacement of the spring from its equilibrium.

Usually the design of the passive spring is set as pre-compressed, which means that when the vehicle is not moving the spring is exerting force in an upward vertical direction [17].

In figure 2.4, the impact that a varying suspension stiffness has on the vehicle in terms of comfort and road grip can be seen.

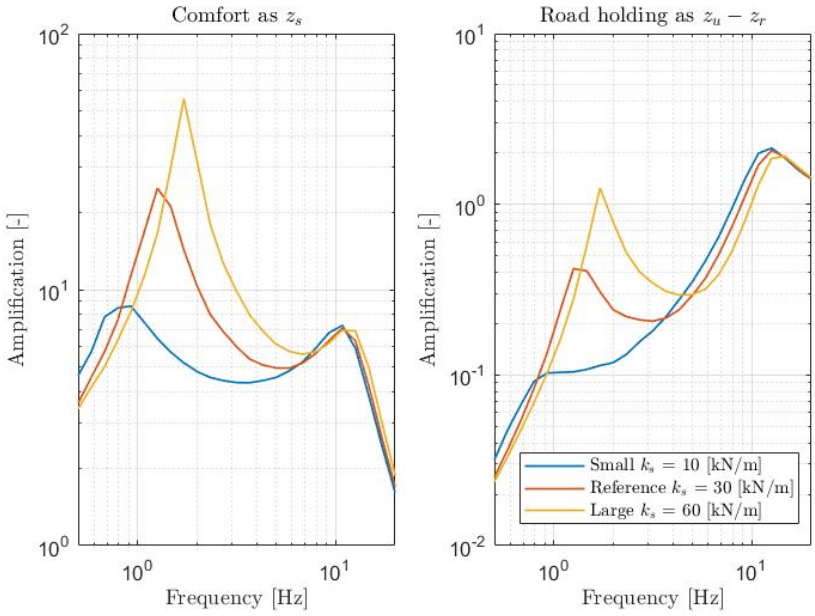

Figure 2.4: *Transfer function from road to vertical displacement (z_s) and road holding ($z_u - z_r$) for varying spring stiffness.*

Increasing the spring stiffness increases the body resonance frequency. In terms of comfort, the transmissibility is increased mainly around the body resonance frequency for an increased spring stiffness. In terms of road holding, an increase in transmissibility for frequencies around the body resonance frequency is seen as well as a slight decrease around the wheel hop frequency, for an increased spring stiffness.

Air suspension

Air suspension is based on replacing the passive spring in a suspension with an air spring. The air springs are able to provide a lower system spring rate than a regular passive spring as well as a lower natural frequency which will lead to improved vibration isolation [6]. The air spring consists of one or two volumes which are made of flexible materials which leads to non-linear behaviour during compression and expansion. With a single volume air spring the stiffness can be assumed to be constant during operation, which can be seen in the ideal gas law:

$$pV = nRT \tag{2.12}$$

Where p is the gas pressure, V is the gas volume, T is the gas temperature, n is the amount of substance of gas and R is the ideal gas constant.

If an extra volume is added to the air spring the spring stiffness will become adjustable to a certain degree, assuming the other parameters are kept constant.

2.4 Control methods

Many control methods for semi-active suspension systems have been researched throughout the years, all with various amount of complexity and performance characteristics. While good results can be achieved with complex methods such as H_∞ control, it does not imply that the results will be better than the less complex ones, as shown in section 1.3.1.

In section 2.4.1 and 2.4.2, some of the simple and more commonly used control strategies are presented. A mix, that has not been as thoroughly tested in earlier research, is presented in section 2.4.3.

2.4.1 Skyhook control

Skyhook theory is based on the vehicle being suspended by a hook in the sky and thus reducing oscillations, caused by the road, independently for the body and wheel. It was first developed by Karnopp et al. [8].

The algorithm for a 2-state Skyhook control is given by:

$$b = \begin{cases} b_{max} & \text{if} \quad \dot{z}_s \dot{z}_{def} > 0 \\ b_{min} & \text{if} \quad \dot{z}_s \dot{z}_{def} \leq 0 \end{cases} \tag{2.13}$$

The parameters b_{max} and b_{min} are the maximum and minimum damping coefficients that the damper can provide at a given damper velocity. and b is the skyhook damping coefficient. $\dot{z}_s$ is the body velocity and $\dot{z}_{def}$ is the suspension deflection.

Skyhook control is seen as a comfort oriented control approach of suspension systems and is commonly used due to its simplicity. While it is not realistic to

have the vehicle being linked to the sky, similar behaviour can achieved for the sprung mass by using the algorithm shown in equation 2.13.

2.4.2 Acceleration driven damper control

Acceleration driver damper (ADD) control was developed by Savaresi et al. [14][15]. The algorithm is similar to the one used for skyhook control, but instead of using the vertical body velocity in the switching law, vertical body acceleration is used.

ADD control has shown improvements in terms of comfort but is not well adapted to road-holding.

$$b = \begin{cases} b_{max} & \text{if} \quad \ddot{z}_s \dot{z}_{def} > 0 \\ b_{min} & \text{if} \quad \ddot{z}_s \dot{z}_{def} \leq 0 \end{cases} \tag{2.14}$$

The parameters b_{max} and b_{min} are the maximum and minimum achievable damping coefficients, b is the ADD damping coefficient and $\ddot{z}_s$ is the body acceleration.

2.4.3 Mixed Skyhook-ADD control

The mixed skyhook-ADD control strategy was introduced by Savaresi et al. [16]. Skyhook control shows improved performance in low frequencies and ADD control for mid to high frequencies, in terms of comfort. By choosing the frequency at which the behaviour is improved for each control strategy, performance can be increased over all frequencies.

The algorithm for mixed skyhook-ADD control is shown by:

$$b = \begin{cases} b_{max} & \text{if} \quad (\ddot{z}_s^2 - \alpha \dot{z}_s^2 \leq 0 \wedge \dot{z}_s \dot{z}_{def} > 0) \vee \\ & \quad\;\; (\ddot{z}_s^2 - \alpha \dot{z}_s^2 > 0 \wedge \dot{z}_s \dot{z}_{def} > 0) \\ b_{min} & \text{if} \quad (\ddot{z}_s^2 - \alpha \dot{z}_s^2 \leq 0 \wedge \dot{z}_s \dot{z}_{def} < 0) \vee \\ & \quad\;\; (\ddot{z}_s^2 - \alpha \dot{z}_s^2 > 0 \wedge \dot{z}_s \dot{z}_{def} < 0) \end{cases} \tag{2.15}$$

The tuning parameter α is the crossover frequency between skyhook and ADD control, b_{max} and b_{min} are the maximum and minimum achievable damping coefficients and b is the mixed skyhook-ADD damping coefficient

The downside with this method is that it is not evaluated as thoroughly as the other previous mentioned control methods. Evaluation of the tuning of α needs to be made in order to properly be able to use this for real world driving.

2.5 ISO classification of road

A road is made up of different combinations of irregularities. One such irregularity can be a pothole or a bump, which can be described as a transient disturbance. In a simulation based environments these disturbances can be modeled as a step or a ramp.

Stationary oscillating disturbances express the undulating nature of the road and can be modeled with sinusoidal waves in the modeling environment. The texture of the surface can be categorized as a random noise input [17].

The road profile can be derived from the following equation:

$$z_r = (m_{us}\ddot{z}_{us} - k_s(z_s - z_{us}) + k_t z_{us} + F_d)/k_t \tag{2.16}$$

where m_{us} is the weight of the unsprung mass, $\ddot{z}_{us}$ is the acceleration of the unsprung mass, k_s is the spring stiffness, z_s and z_{us} are the displacements of the sprung and unsprung masses, k_t is the tire stiffness and F_d is the damper force.

In ISO 8608 would a road be classfied according to the highest amplitude over the spatial frequency spectra. The spatial frequency spectra is useful in order to determine the ISO class of a road since the road can be classified identically no matter the speed of the vehicle. The ISO class is determined according to the PSD of the road and is defined by:

$$\Phi(\Omega) = \Phi_0 \left(\frac{\Omega}{\Omega_0} \right)^{-w} \tag{2.17}$$

Where Ω_0 is the spatial frequency reference, set to 1. $\Phi(\Omega)$ is the PSD at the spatial frequency Ω and w is the road waviness. Smooth roads has larger road waviness than rough roads. ISO 8608 uses a waviness factor of 2. Φ_0 is the reference PSD for different road classifications, seen in table 2.1

Table 2.1: *Road classification*

Road class	$\Phi_0 E - 6m^3$
A	16
B	64
C	256
D	1024
E	4096
F	16384

Where a road with ISO class A would be referred to as a smooth road and a road with ISO class F would be referred to as a rough road.

Equation 2.17 can be transformed to the time domain as follows:

$$\Phi(f) = \frac{1}{v}\Phi(\Omega) = \Phi_0 \Omega_0^2 \frac{v}{f^2} \tag{2.18}$$

Where v is the vehicle speed and f is the frequency in Hertz.

3

Controller implementation

This chapter consists of modeling of the damper controller.

3.1 Controller description

A skyhook controller was built with added modifications from Stamatov et al. [18] in order to reduce the jerk motions of the vehicle, based on the requests of Volvo Cars. In figure 3.1 a block diagram of the controller (orange area) and the damper (blue area) can be seen.

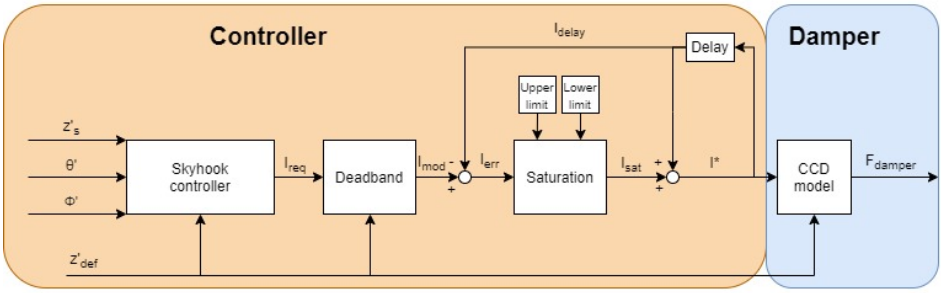

Figure 3.1: *Block diagram of the skyhook controller and added modifications together with the damper.*

The skyhook controller sends out a current request, I_{req}, that is based on the

heave, $\dot{z}$, pitch, $\dot{\Theta}$, and roll, $\dot{\Phi}$, velocities further explained in section 3.1.1. The deadband block is the modulation curve, further explained in section 3.1.2, which makes sure that no force request is sent to the damper when the damper velocity is low. The signal output from the deadband block, I_{mod}, is then reduced with the current that was sent to the damper in the previous time step I_{delay}, which gives the signal I_{err}. If the current request in the previous time step is the same as in the current time step, I_{err} will be zero and no additional current will be sent to the damper. I_{err} is then passed through the saturation block that limits the current being sent to the damper, which is explained in section 3.1.3. Depending on what the upper and lower limit of the saturation block is set to, the rate of change during increase and decrease of current request can be limited. The saturated output signal, I_{sat}, is then added with the the signal from the previous time step, I_{delay}, which gives the final output signal of the controller I^*. The current signal is then sent to the continuously controlled damper (CCD) model, further explained in section 3.2, which sends out a damper force, based on the damper velocity and current request.

3.1.1 Skyhook controller implementation

The skyhook controller is based on the sprung mass velocity, as shown in section 2.4.1. The sprung mass displacement is dependent on the heave displacement, pitch angle and roll angle as shown by:

$$z_{s,FR} = z_s - l\Phi - w\Theta \tag{3.1}$$

$$z_{s,FL} = z_s - l\Phi + w\Theta \tag{3.2}$$

$$z_{s,RR} = z_s + l\Phi - w\Theta \tag{3.3}$$

$$z_{s,RL} = z_s + l\Phi + w\Theta \tag{3.4}$$

Where FR is the front right wheel, FL is the front left wheel, RR is the rear right wheel and RL is the rear left wheel. z_s is the heave displacement, Φ is the pitch angle and Θ is the roll angle. w is half of the track width, or the distance between the center of gravity to the right and left side of the vehicle. l is the mean distance from the center of gravity to the front and rear axis.

The vertical velocity at each corner of the car body can then be calculated by taking the derivative of 3.1-3.4:

$$\dot{z}_{s,FR} = \dot{z}_s - l\dot{\Phi} - w\dot{\Theta} \tag{3.5}$$

$$\dot{z}_{s,FL} = \dot{z}_s - l\dot{\Phi} + w\dot{\Theta} \tag{3.6}$$

$$\dot{z}_{s,RR} = \dot{z}_s + l\dot{\Phi} - w\dot{\Theta} \tag{3.7}$$

$$\dot{z}_{s,RL} = \dot{z}_s + l\dot{\Phi} + w\dot{\Theta} \tag{3.8}$$

The heave velocity and angular velocities of the pitch and roll can be converted to heave force, pitch torque and roll torque through a lookup table, shown in figure

3.2. The lookup table can be modified, depending on the current drivemode desired by the driver. The heave force, pitch torque, and roll torque are thus functions of their velocites as:

$$F_{heave}(\dot{z}_s) \tag{3.9}$$

$$T_{pitch}(\dot{\Phi}) \tag{3.10}$$

$$T_{roll}(\dot{\Theta}) \tag{3.11}$$

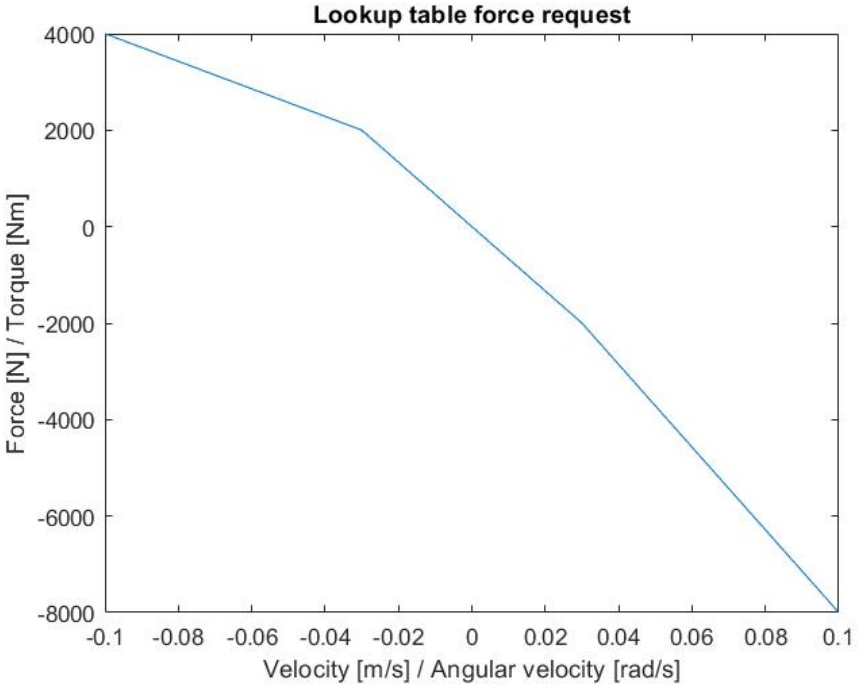

Figure 3.2: *Force and torque based on the heave velocity and angular velocity of pitch and roll.*

The torques caused by the pitch and roll, T_{pitch} and T_{roll}, can be converted to forces at each wheel, using Newton's second law of motion, as follows:

$$\underbrace{-\frac{T_{pitch}}{4l}}_{F_{pitch,FR}} \underbrace{-\frac{T_{pitch}}{4l}}_{F_{pitch,FL}} \underbrace{+\frac{T_{pitch}}{4l}}_{F_{pitch,RR}} \underbrace{+\frac{T_{pitch}}{4l}}_{F_{pitch,RL}} = 0 \tag{3.12}$$

$$\underbrace{-\frac{T_{roll}}{4w}}_{F_{roll,FR}}\underbrace{+\frac{T_{roll}}{4w}}_{F_{roll,FL}}\underbrace{-\frac{T_{roll}}{4w}}_{F_{roll,RR}}\underbrace{+\frac{T_{roll}}{4w}}_{F_{roll,RL}} = 0 \tag{3.13}$$

Where w is the track width divided by two and l is the mean value of l_f and l_r.

Added damping for the front wheels is desired during breaking. The pitch forces are thus acquired as follows:

$$\hat{F}_{pitch,FR} = (1 + K_{pitch})F_{pitch,FR} \tag{3.14}$$

$$\hat{F}_{pitch,FL} = (1 + K_{pitch})F_{pitch,FL} \tag{3.15}$$

$$\hat{F}_{pitch,RR} = (1 - K_{pitch})F_{pitch,RR} \tag{3.16}$$

$$\hat{F}_{pitch,RL} = (1 - K_{pitch})F_{pitch,RL} \tag{3.17}$$

The parameter K_{pitch} is the gain value for the pitch forces, set to 0.1.

The forces caused by the heave movements, acquired from the lookup table seen in figure 3.2, can be divided for the semi-active dampers at the wheels as:

$$F_{heave} = \underbrace{\frac{F_{heave}}{4}}_{F_{heave,FR}}\underbrace{+\frac{F_{heave}}{4}}_{F_{heave,FL}}\underbrace{+\frac{F_{heave}}{4}}_{F_{heave,RR}}\underbrace{+\frac{F_{heave}}{4}}_{F_{heave,RL}} \tag{3.18}$$

More damping is desired during rebound. Thus, the forces for heave, roll and pitch can be acquired such as:

$$\bar{F}_{heave} = \begin{cases} K_{compr}F_{heave} & \text{if} \quad F_{heave} \geq 0 \\ K_{rebound}F_{heave} & \text{if} \quad F_{heave} < 0 \end{cases} \tag{3.19}$$

$$\bar{F}_{pitch} = \begin{cases} K_{compr}\hat{F}_{pitch} & \text{if} \quad \hat{F}_{pitch} \geq 0 \\ K_{rebound}\hat{F}_{pitch} & \text{if} \quad \hat{F}_{pitch} < 0 \end{cases} \tag{3.20}$$

$$\bar{F}_{roll} = \begin{cases} K_{compr}F_{roll} & \text{if} \quad F_{roll} \geq 0 \\ K_{rebound}F_{roll} & \text{if} \quad F_{roll} < 0 \end{cases} \tag{3.21}$$

Where K_{compr} is the compression gain, set to 0.6, and $K_{rebound}$ is the rebound gain, set to 1.4.

The semi-active damper at each wheel will then recieve a force request such as:

$$F_{req} = max(\bar{F}_{heave}, \bar{F}_{pitch}, \bar{F}_{roll}) \tag{3.22}$$

Where F_{req} is the force request that is sent to the damper. By having the largest force be selected by the controller, different disturbances be attenuated separately e.g. roll forces during cornering or pitch forces during breaking.

By varying the requested force from the controller, different forces can be re-

quested at each wheel. Increasing or decreasing the force requests from the controller will further be referred to as **force gain control** and is shown by:

$$\hat{F}_{req} = K_{force} F_{req} \tag{3.23}$$

Where K_{force} is the force gain.

The damping coefficient in equation 2.13 is a function of force and damper velocity such as:

$$b = \frac{F}{\dot{z}_{def}} \tag{3.24}$$

Which gives the possibility of rewriting equation 2.13 as:

$$\bar{F}_{req} = \begin{cases} \hat{F}_{req} & \text{if} \quad \dot{z}_s \dot{z}_{def} > 0 \\ F_{min} & \text{if} \quad \dot{z}_s \dot{z}_{def} \leq 0 \end{cases} \tag{3.25}$$

Where $\hat{F}_{req}$ is the requested force and F_{min} is the minimum possible damper force for a given damper velocity $\dot{z}_{def}$.

Since an actual damper takes a current as input is the force request converted to a current based on the damper velocity. The current is a function of force request and damper velocity as follows:

$$I_{req}(\bar{F}_{req}, \dot{z}_{def}) \tag{3.26}$$

The currents for the dampers at each wheel are acquired through an inverse of the lookup table shown in figure 3.5.

In order to make sure that the minimum possible damping is provided for cases outside of the damper working region is the current clamped to the minimum possible current for cases outside of the damper working region such as:

$$\hat{I}_{req} = \begin{cases} I_{req} & \text{if} \quad \dot{z}_s \dot{z}_{def} > 0 \\ I_{min} & \text{if} \quad \dot{z}_s \dot{z}_{def} \leq 0 \end{cases} \tag{3.27}$$

Where I_{req} is the requested current and I_{min} is the minimum possible current. The current request, $\hat{I}_{req}$, is thus the final output of the controller.

3.1.2 Deadband implementation

In order to smoothen out the force delivery during changes in damper working region, a modulation curve, or deadband, of the current request was implemented. Stamatov et al. [18] evaluated this method and came to the conclusion that the peak jerk values could be drastically reduced while keeping the advantages of skyhook control. The algorithm is based on the damper velocity $\dot{z}_{def}$ and the force request F_{req}, which indirectly affects the current request I_{req}, as mentioned in section 3.1.1.

When either $\dot{z}_{def}$ or F_{req} changes sign and the working region of the damper is either entered or exited, the modulation curve allows for a soft transition of the

current signal, I_{req}. The equation for the modulation curve is:

$$g(x) = \begin{cases} 2\left(\frac{x}{L(1+\alpha)}\right)^n & \text{if} \quad 0 < x < L\alpha \\ 2\frac{\alpha + \frac{x/L-\alpha}{1+\left(\frac{x/L-\alpha}{1-\alpha}\right)^2}}{1+\alpha}^n & \text{if} \quad L\alpha < x < L \\ 1 & \text{if} \quad x > L \end{cases} \tag{3.28}$$

Where $0 < \alpha < L$ and $n \geq 1$. Which gives the modulated current signal, I_{mod}, as follows:

$$I_{mod} = I_{req} g(\dot{z}_{def}) \tag{3.29}$$

By varying the parameters different characteristics of the curve will be achieved, as shown in figure 3.3.

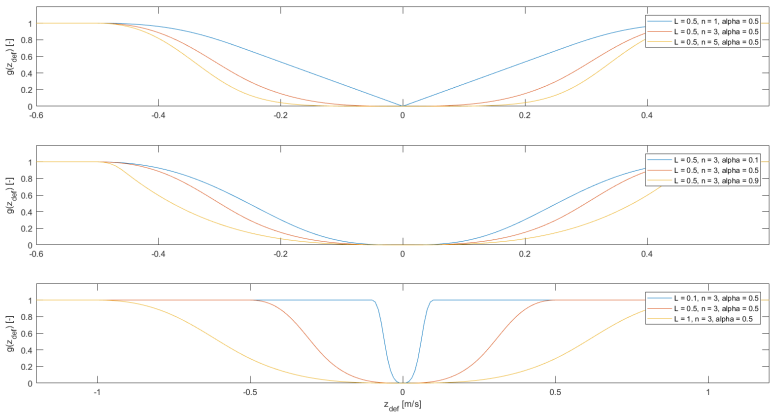

Figure 3.3: *Modulation curve for different parameter values.*

L is the parameter that defines the range in which the signal will be modulated i.e. for an L value of 0.5 would the signal be modulated for damper velocities inside the range of ±0.5m/s, while damper velocities above or below ±0.5m/s would remain unchanged.

3.1.3 Rate limit implementation

Stamatov et al. [18] also suggested that a rate of change limiting of the control signal was to be implemented in the model in order to further improve the vehicle jerk. In figure 3.1, this is shown as the saturation block.

In figure 3.4 a step response from 0A to 1.6A is shown with varying rate limits.

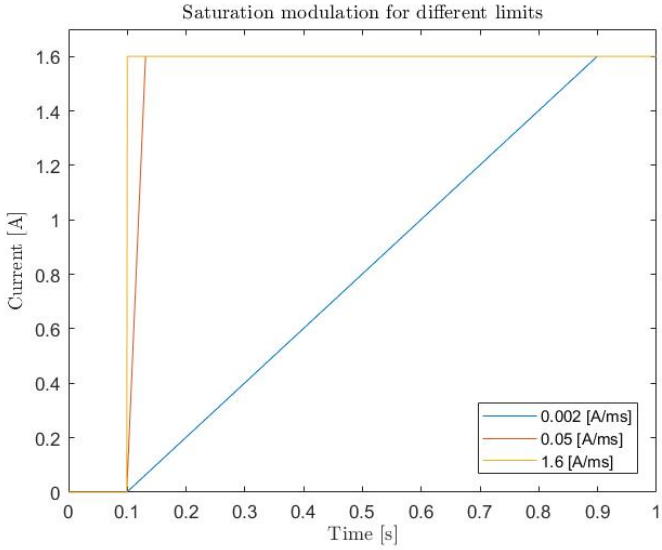

Figure 3.4: *Plot of current over time for varying rate limitations.*

Thus when the rate limit is changed a different amount of damping will be achieved. Varying the rate limits will further be referred to as **rate limitation control**.

3.2 Continuously controlled damper model

A continuously controlled damper (CCD) model was implemented to replicate the physical behaviour of the semi-active damper. The force output from the CCD model is based on the damper velocity and the current output from the controller such as:

$$F_{damper}(I^*, \dot{z}_{def}) \tag{3.30}$$

Where F_{damper} is the damper force, I^* is the current input to the CCD model and $\dot{z}_{def}$ is the damper velocity. Thus, the force output is a function of damper velocity and current input. The damper force is provided through a lookup table of the damper characteristics, as shown in figure 3.5.

The semi-active rule of damping states that damping can only be provided in the opposite direction of the damper velocity and always needs to be taken into consideration when designing a damper model. In the skyhook controller shown in section 3.1.1, the semi-active rule of damping is handled through clamping of current down to the minimum possible current which means that for cases outside of the damper working region, the CCD model will output a minimum damper force for a given damper velocity. Due to the limitations in semi-active dampers, caused by a limited bandwidth, a bandwidth was introduced at about 50Hz.

The model is also designed with an increased amount of damping during rebound in comparison to during compression. This behaviour is desired due to scenarious where the vehicle is driven over a steep bump and low damping is wanted in order to reduce the jerk motion of the vehicle. In the other end of the spectrum, where the vehicle is driven over a pot hole, high damping is desired in order to decrease downward jerk in the vehicle.

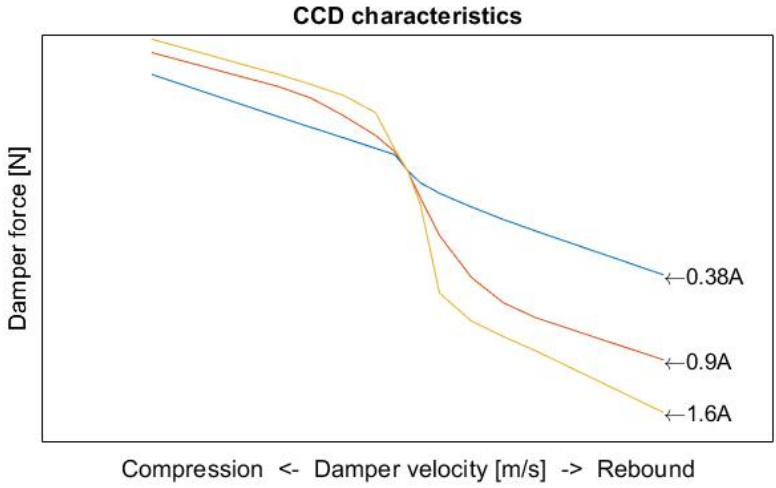

Figure 3.5: *CCD damper force as a function of damper velocity and current*

4

Quarter car model simulation

This chapter consists of the modeling of a quarter car model together with tests carried out on the quarter car model with the controller that was built in chapter 3.

4.1 Quarter car model

Quarter car modeling is a common way to analyze vehicle dynamics. Despite simplifying the car to a 2DOF model the main characteristics (dynamic tire force, body acceleration and suspension working space) to suspension performance can be assessed. The model consists of a sprung mass, m_s, which represents a quarter of the body of the vehicle along with an unsprung mass, m_{us}, which represents the suspension and wheel. These masses are connected through a spring with the stiffness coefficient k_s and a variable damper with the damping coefficient b_s. When the wheel is in contact with the ground the tire characteristics will cause it to act as a spring with the coefficient k_t. The road disturbance is described by the variable z_r. The quarter-car suspension can be seen in figure 4.1.

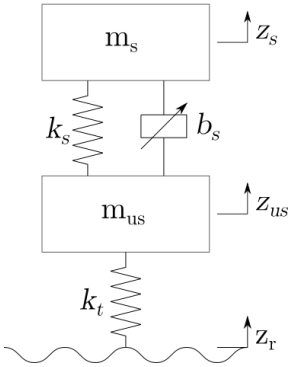

Figure 4.1: *Quarter car model*

The equations of motion for the quarter car model are:

$$m_s\ddot{z}_s + k_s z_{def} + b_s\dot{z}_{def} = 0 \tag{4.1}$$

$$m_{us}\ddot{z}_{us} - k_s z_{def} - b_s\dot{z}_{def} + k_t(z_{us} - z_r) = 0 \tag{4.2}$$

where $\ddot{z}_s$ and $\ddot{z}_{us}$ represents the acceleration of the sprung- and unsprung mass. $z_{def} = z_s - z_{us}$ and $\dot{z}_{def} = \dot{z}_s - \dot{z}_{us}$ represents the position and velocity of the suspension deflection and z_r is the road disturbance position.

The quarter car was modeled in Simulink and can be seen in figure 4.2.

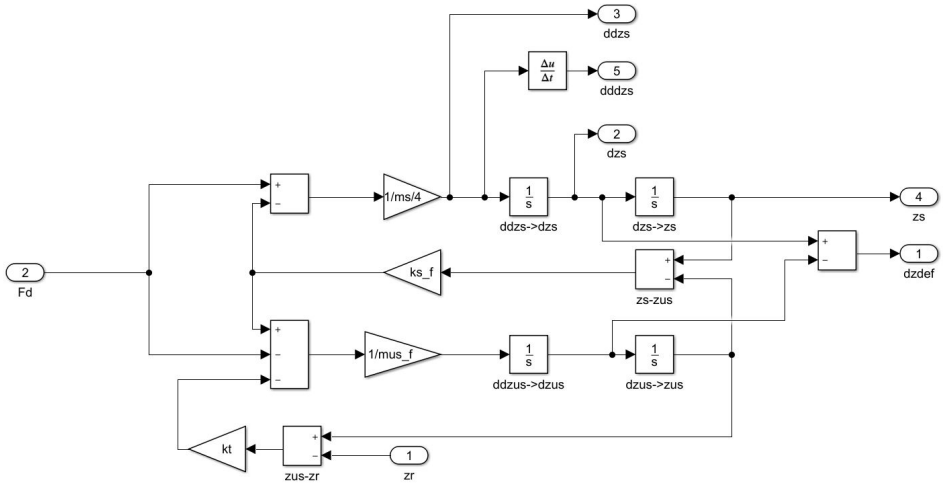

Figure 4.2: *Quarter car model in Simulink*

4.2 Test cases

In this section, tests of the model described in section 3.1 will be made with the quarter car model from section 4.1 for high and low frequency scenarios. For each scenario, five cases will be tested against each other. In order to assure that rate limit control is a valid control method, since no explicit research in the area has been made, is it going to be compared for three different rate limits. To assess the validity of the research that Stamatov et al. [18] conducted will tests also be made against skyhook control without a deadband and rate limit. The results will also be compared against a regular passive damping.

These cases are summarized as follows:

- **Passive suspension**: Passive damping
- **Reference**: Skyhook damping with deadband and rate limit. Upper rate limit set at 0.05A/ms.
- **Increased**: Skyhook damping with deadband and rate limit. Upper rate limit set at 0.1A/s.
- **Decreased**: Skyhook damping with deadband and rate limit. Upper rate limit set at 0.002A/s.
- **Skyhook**: Skyhook damping without deadband and rate limit.

All tests were made with the modulation curve parameters from equation 3.28 set to $L = 0.1$, $n = 3$, $\alpha = 0.5$ and the lower rate limit set to -1.6A/ms.

4.2.1 Low frequency response

In this case the input was set as a sine wave with amplitude 0.05m and frequency 2Hz. In figure 4.3 the RMS values of body acceleration can be seen, which shows that all semi-active control methods provide better ride comfort than the passive suspension for low frequencies.

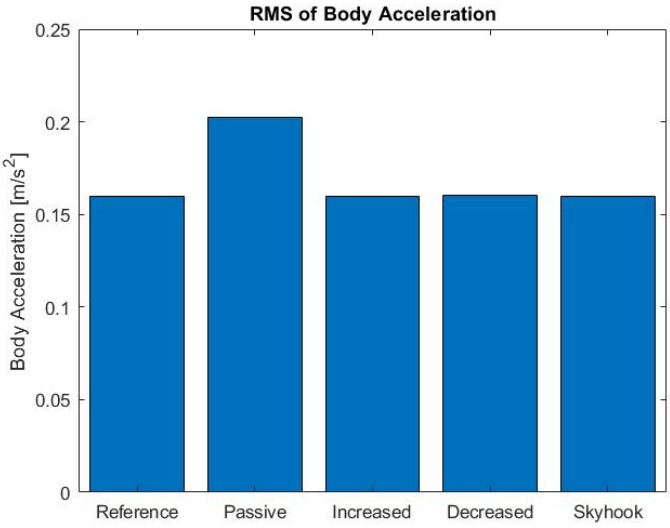

Figure 4.3: *RMS values of body acceleration for the low frequency response*

Figure 4.4 shows the peak jerk values for each control method. It can be seen that all of the varying rate limit cases provides decreased peak jerk values compared to the skyhook control. The relatively low peak jerk value for the passive suspension comes down to how these are designed in order to give the best behaviour during common driving scenarios and repeating movements.

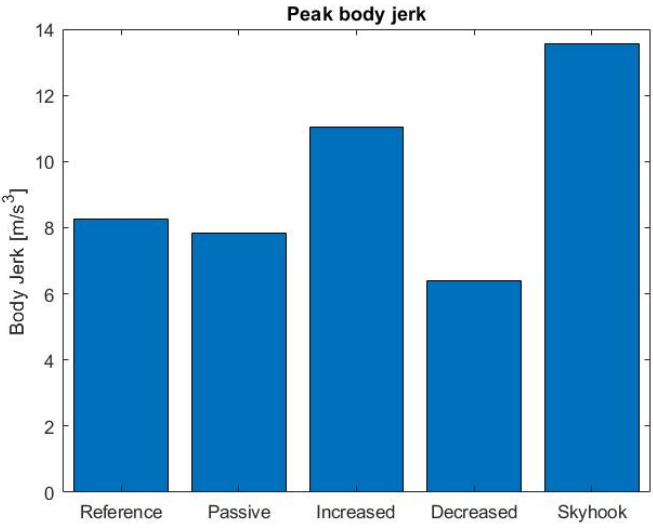

Figure 4.4: *Peak jerk values for the low frequency response*

4.2.2 High frequency response

For the high frequency response a sine wave with amplitude 0.05 and frequency 10Hz was used as road input. The RMS values of body acceleration can be seen in figure 4.5 and shows similar behaviour, with a slight improvement for the semi-active control methods compared to the passive case.

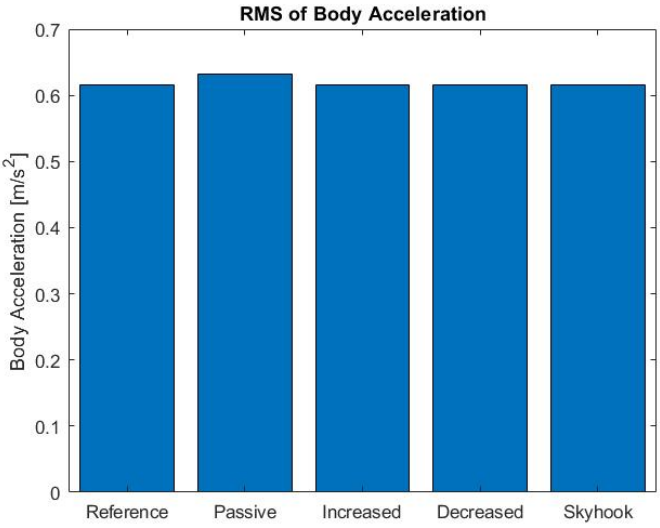

Figure 4.5: *RMS values of body acceleration for the high frequency response*

In figure 4.6, the clear improvements for the semi-active suspensions compared to the passive suspension are shown as the peak jerk values for all semi-active control methods are less than half of the passive suspension.

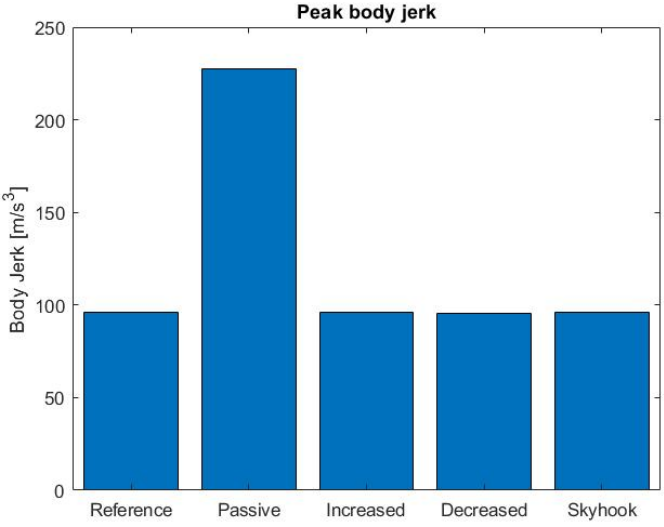

Figure 4.6: *Peak jerk values for the high frequency response*

4.2.3 Response of entire frequency spectra

In order to evaluate the entire frequency spectra, a chirp wave which gradually increased from 0.1Hz to 30Hz with 0.05m amplitude, was used as road input. In figure 4.7 a PSD plot of body acceleration can be seen.

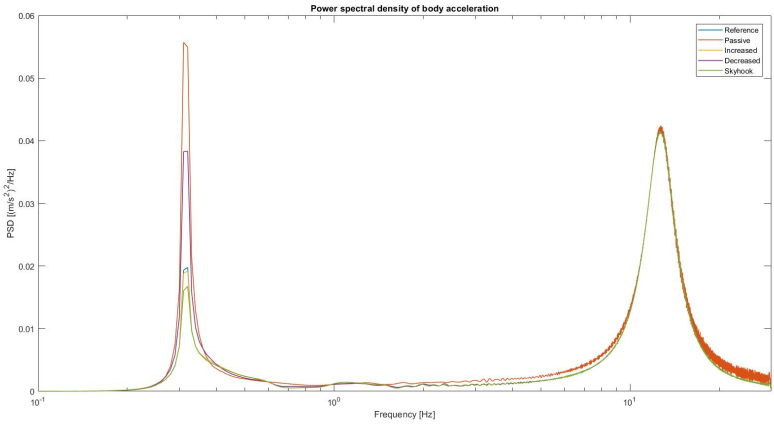

Figure 4.7: *PSD plot of body acceleration for 0.1 to 30Hz*

While skyhook control does give the best result in terms of ride comfort around body resonance frequency it can be seen that the model with deadband and rate limit gives similar results for all frequencies. Although the body acceleration is slightly worsened with the varying rate limit, a decrease in peak jerk was achieved, as shown in section 4.2.1. It can also be seen that both the skyhook control and skyhook control with varying rate limits give better performance for all frequencies up to the wheel hop frequency.

5

Full car model simulation

In this chapter different control methods will be compared and evaluated for different roads in terms of ride comfort and road holding through simulations in IPG Carmaker.

5.1 IPG Carmaker

Carmaker is a software tool used for virtual testing of vehicles. For the test runs certain parameters needs to be adjusted and is explained below.

- Vehicle data set: Parameters such as body weight, trackwidth and tire stiffness needs to be set.
- Sensors: Sensors can be placed at various locations of the vehicle which can then be read in Simulink.
- Maneuver: The behaviour of the vehicle is set, which can include acceleration, breaking and road offset.
- Road/scenario: Roads can either be created from scratch where the length is set and various disturbances are created manually, such as bumps or turns. For the cases tested in this thesis, the roads were imported as bumps which allowed for creating roads that represented real-life scenarios, i.e. low- and high frequency disturbances.

5.2 Test cases

The control methods that will be compared are force gain control, explained in section 3.1.1 as well as rate limitation control, explained in section 3.1.3. By

varying the amount of force gain, the requested force signal will change and thus result in a change of damping. A change in rate limitation will only change the rate at which current is applied to the damper.

1. **Varying force gain**
   - Force gain = 0.5 [-]
   - Force gain = 0.75 [-]
   - Force gain = 1 [-]

   For the test cases with varying force gain the rate limitation was set to 0.05 A/ms.

2. **Varying rate limitation**
   - Rate limit = 0.001 [A/ms]
   - Rate limit = 0.5 [A/ms]
   - Rate limit = 1.6 [A/ms]

   For the test cases with varying rate limit the force gain was set to 1.

   The characteristics of an air spring and a passive spring aren't identical, as mentioned in section 2.3.3. Similar results can however be achieved if the nonlinearity of the air spring is ignored. For the purpose of this thesis the adjustable stiffness of the air spring will be simulated with a variation of the passive spring stiffness.

3. **Varying spring stiffness**
   - Spring stiffness gain = 1 [-] (below referred to as "Force gain = 1")
   - Spring stiffness gain = 0.75 [-]

The spring stiffness gain refers to percentage of the reference stiffness. Thus does 0.75 equal 75% of the reference stiffness.

All tests were made with the modulation curve parameters from equation 3.28 set to $L = 0.1, n = 3, \alpha = 0.5$. The lower rate limit was set to -1.6A/ms and the sampling frequency was 1000Hz. The simulated vehicle was driven at 70km/h with a 70kg load for all test cases.

5.2.1 Road A

In figure 5.2 the road profile for road A can be seen for the right and left side of the vehicle. The road profile for each side is relatively similar, which means that the main forces that will act on the vehicle are caused by heave and pitch movements with minimal roll forces. The road consists of both right and left curves.

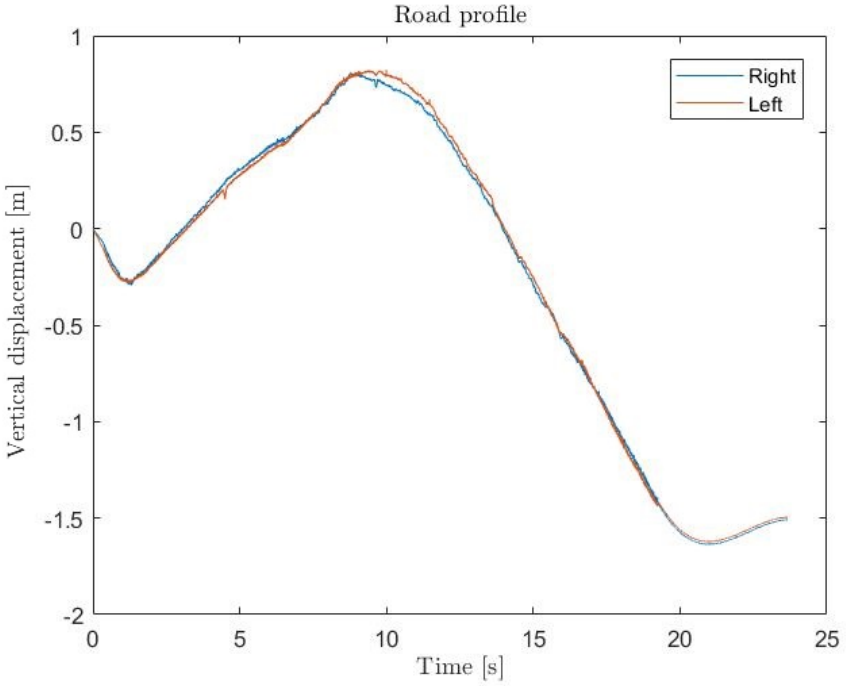

Figure 5.1: *Road profile of road A*

Figure 5.2 shows the PSD plot of road displacement for spatial frequencies in the range of 0.02 cycles/m to 4 cycles/m, which equates to approximately 0.4Hz to 78Hz for a vehicle driven at 70km/h (19.4m/s). This road has similar low and high frequency content and would be classified as an ISO-D class for high frequencies, seen in figure 5.2.

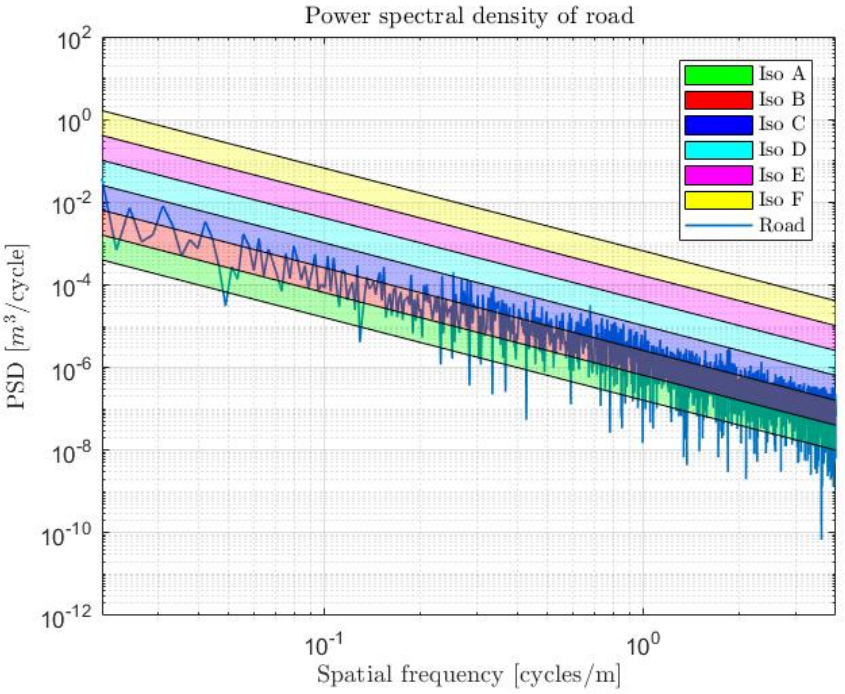

Figure 5.2: *PSD plot of road A for the right side of the vehicle with ISO classification*

Table 5.1 shows the comfort measures of RMS of body acceleration over three different frequency spectra, peak jerk values as well as the RMS values of the tire deflection. The respective PSD plots for body acceleration and tire deflection can be seen in appendix A.

Table 5.1: *Comfort and road holding values for road A*

	RMS $\ddot{z}_s$ [m/s^2]			Peak jerk [m/s^3]	RMS z_{def_t} [m]
	1-4Hz	4-8Hz	8-20Hz	-	0.5-30Hz
Force gain = 0.5	0.389	0.171	0.305	3764	0.00216
Force gain = 0.75	0.367	0.192	0.311	5175	0.00211
Force gain = 1	0.349	0.191	0.322	3733	0.00209
Rate limit = 0.001	0.415	0.166	0.284	4306	0.00223
Rate limit = 0.5	0.328	0.203	0.323	5745	0.00208
Rate limit = 1.6	0.339	0.215	0.338	3763	0.00216
Spring gain = 0.75	0.281	0.177	0.325	3543	0.0021

It can be seen that the lowered force gain improves ride comfort in both the

medium and high frequency spectra. The lowered force gain also results in a slightly worsened road holding ability for frequencies in the range of 0.5-30Hz.

For low frequencies, a clear decrease in ride quality can be seen for the lowered rate limits. For the medium and high frequency range a significant improvement can however be seen in terms of RMS of body acceleration. Similar to the force gain cases, the road holding get worsened with the lowest rate limit, but does appear to give a slight improvement when the rate limit is set to 0.5 compared to 1.6.

Comparing the the reference case, where force gain is set to 1, with the lowered spring stiffness, where the only parameter differing is the spring stiffness, an improvement in ride comfort can be seen for low and medium frequencies with a slight decrease for high frequencies. The lowered spring gain also results in a worsened road holding ability for frequencies in the range 0.5-30Hz.

It is interesting to note that there doesn't appear to be a linear correlation between the peak jerk values and the different control methods.

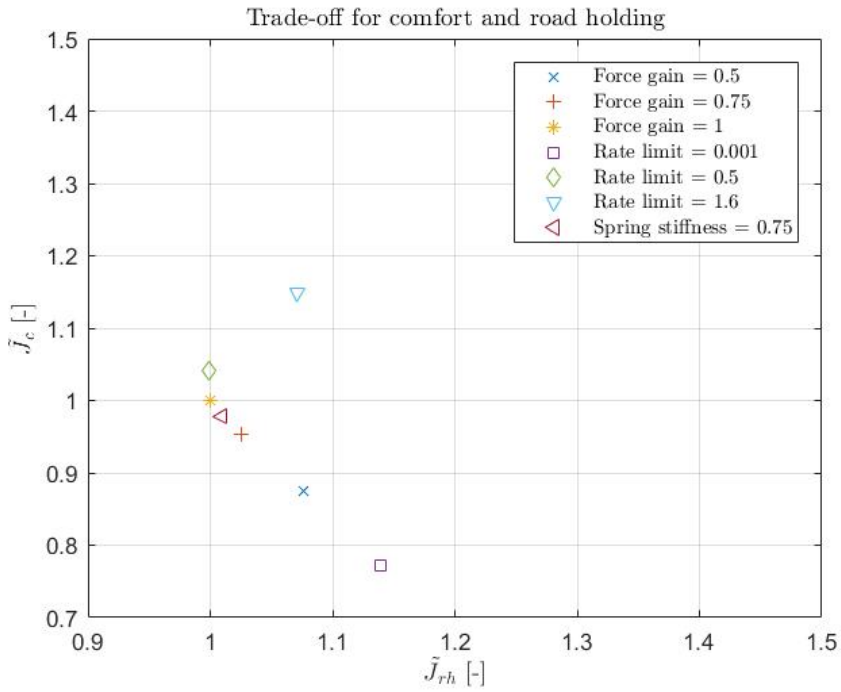

Figure 5.3: *Trade-off between road holding and comfort with force gain set to 1 as reference*

In figure 5.3 the comfort and road holding parameters $\tilde{J}_c$ and $\tilde{J}_{rh}$, calculated as explained in section 2.2.5, are plotted against eachother. It can be seen that the best

road holding ability is achieved with force gain set to 1. The trade-off between road holding and comfort appears clearly for the cases with lowered force gain and rate limit set to 0.001, where the best comfort is also achieved.

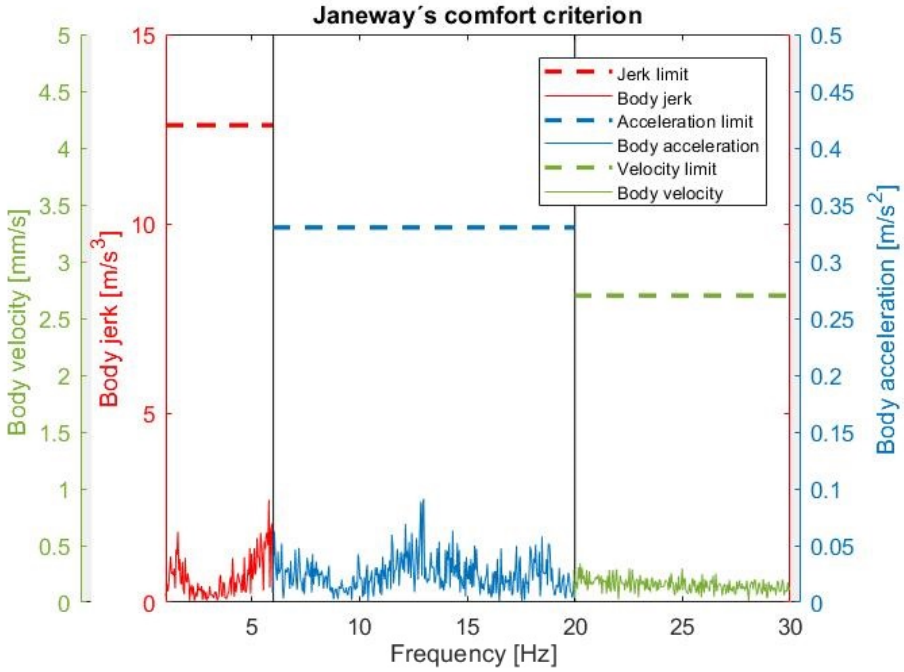

Figure 5.4: *Janeway's comfort criterion for rate limit set to 1.6*

In figure 5.4 the body jerk, body acceleration and body velocity for the worst test case in terms of comfort, rate limit set to 1.6, are plotted over the frequency intervals 1-6Hz, 6-20Hz and 20-30Hz with it's respective limits according to Janeway. It can be seen that even for the worst test case, the comfort is still well within the range of comfort, according to Janeway.

5.2.2 Road B

In figure 5.5 the road profile of road B can be seen. The road profile is rather similar for both sides of the vehicle but with an offset of 5cm which will cause some roll forces on the vehicle. The shape of road B is straight.

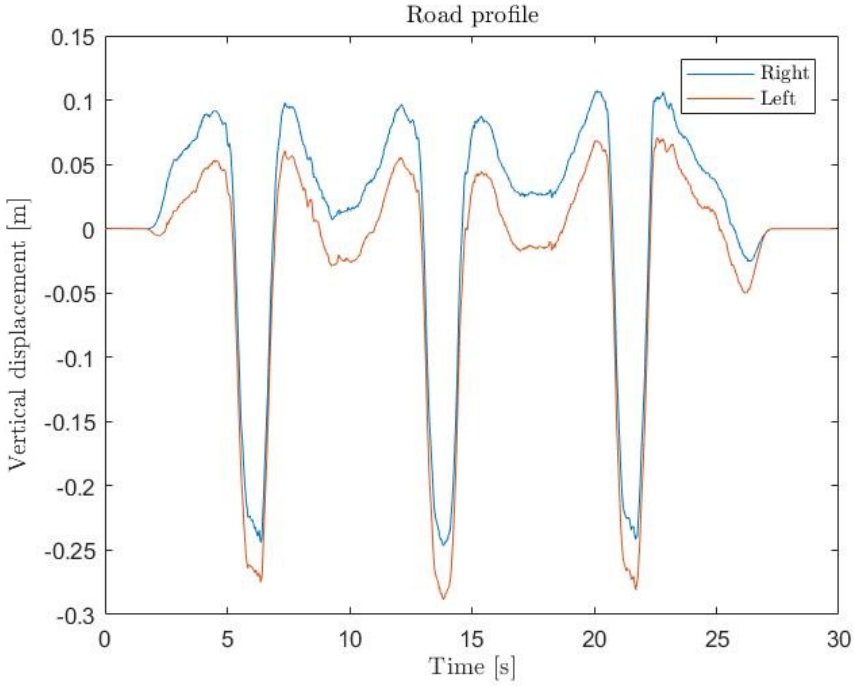

Figure 5.5: *Road profile of road B*

In the PSD plot of the road, shown in figure 5.6, it can be seen that the frequency content for low frequencies are dominant. This road would be classified as ISO-E for low frequencies.

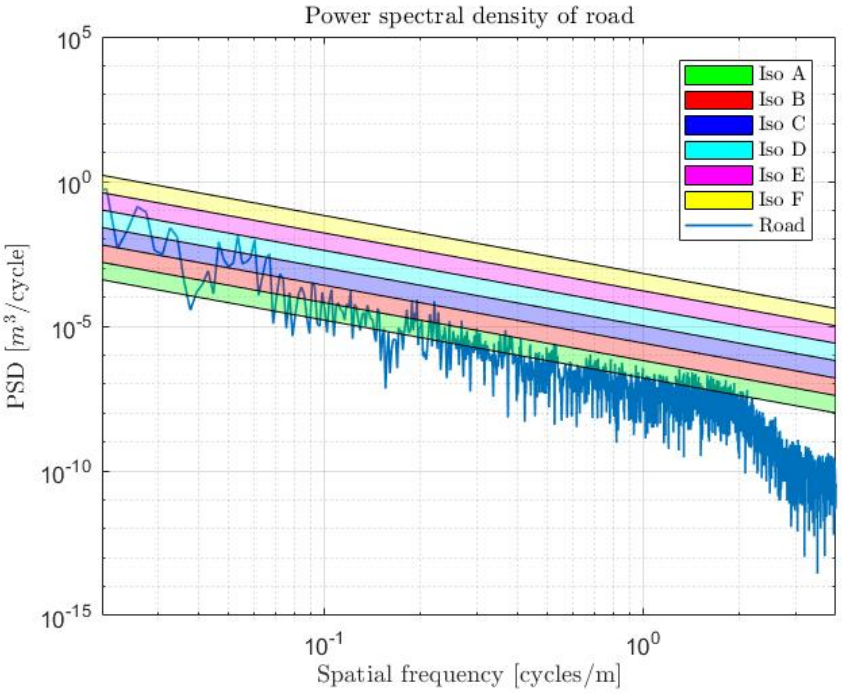

Figure 5.6: *PSD plot of road B for the right side of the vehicle with ISO classification*

Table 5.2 shows the comfort measures of RMS over three different frequency spectra, peak jerk values as well as the RMS values of tire deflection. The respective PSD plots for body acceleration and tire deflection can be seen in appendix B.

Table 5.2: *Comfort and road holding values for road B*

	RMS $\ddot{z}_s$ [m/s^2]			Peak jerk [m/s^3]	RMS z_{def_t} [m]
	1-4Hz	4-8Hz	8-20Hz	-	0.5-30Hz
Force gain = 0.5	0.947	0.104	0.096	129	0.00169
Force gain = 0.75	0.905	0.123	0.099	201	0.00161
Force gain = 1	0.893	0.128	0.101	192	0.00157
Rate limit = 0.001	1.098	0.08	0.085	153	0.00189
Rate limit = 0.5	0.89	0.128	0.102	252	0.00157
Rate limit = 1.6	0.89	0.128	0.102	251	0.00157
Spring gain = 0.75	0.887	0.117	0.1	186	0.00142

In figure 5.7 the trade-off between road holding and comfort can be seen for road B. Both road holding and comfort is improved with lowered spring stiffness.

Increasing the rate limits led to a slight improvement in road holding, but is barely noticable. The lowered force gains and lowered rate limit all led to large trade-off between comfort and road holding.

Due to the the small amount of high frequency disturbances it can be seen that the peak jerk values are relatively small.

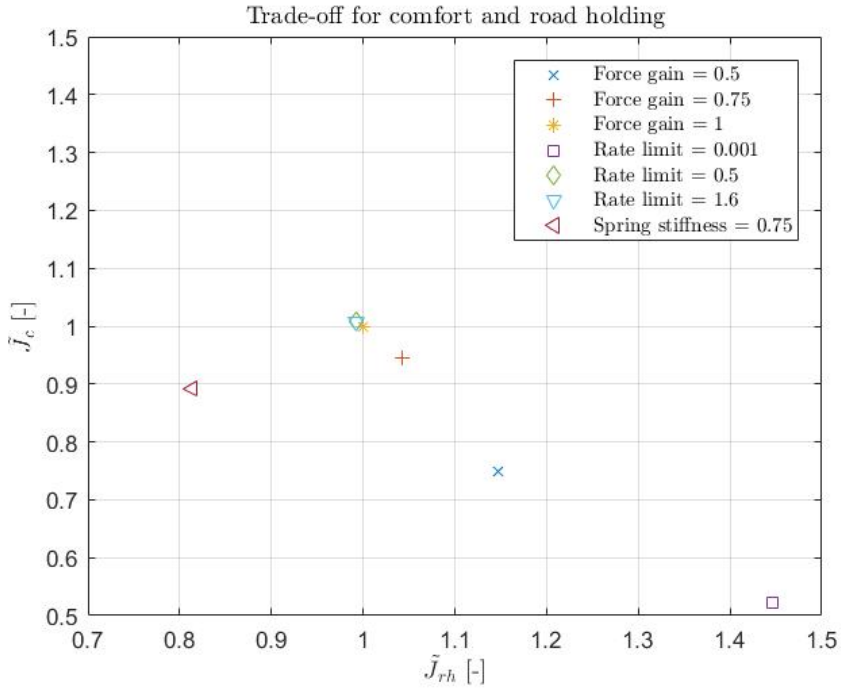

Figure 5.7: *Trade-off between road holding and comfort with force gain set to 1 as reference*

The worst comfort was achieved when the rate limit was set to 0.5. When compared to Janeway's comfort criterion, seen in figure 5.8, it can be seen that it is still well within the limits.

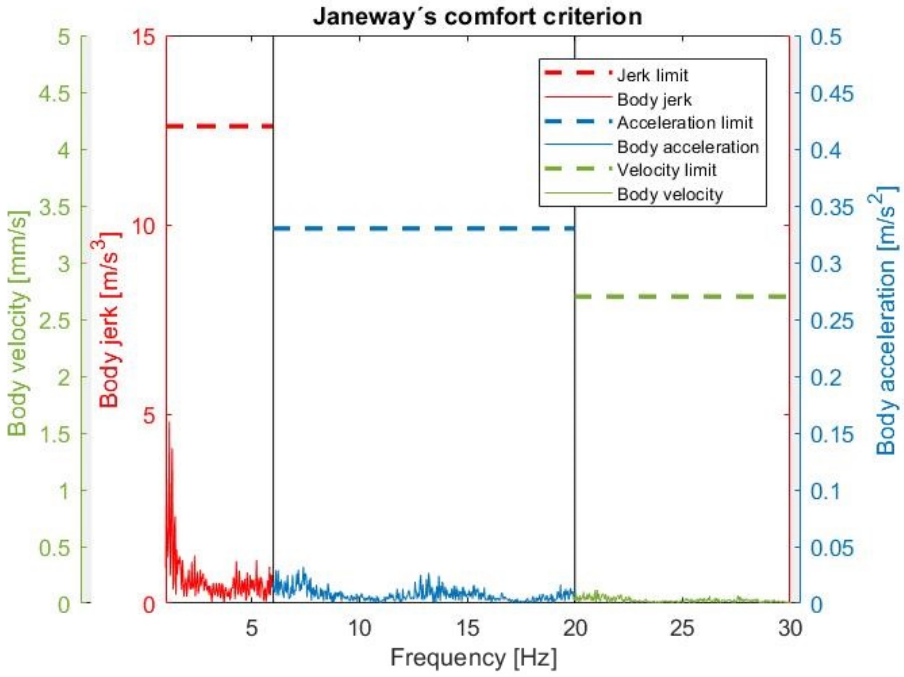

Figure 5.8: *Janeway's comfort criterion for rate limit set to 0.5*

5.2.3 Road C

The road profile for the straight road C can be seen in figure 5.9. Due to the height differences for each side of the vehicle, roll forces will be exerted to the vehicle.

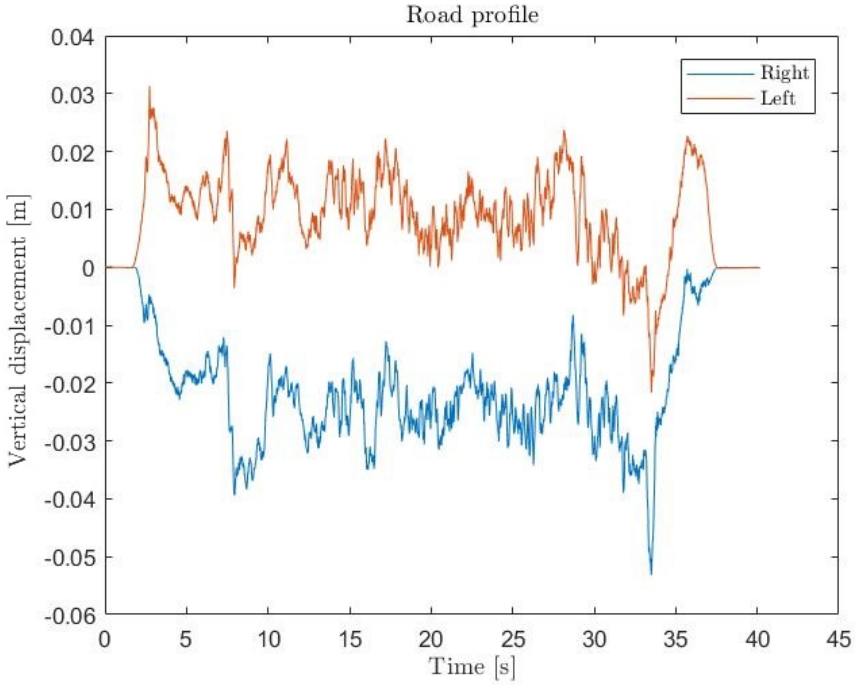

Figure 5.9: *Road profile of road C*

In figure 5.10 the PSD plot for the right side of the vehicle can be seen. The road is similar to road B, but with a smaller amplitude for the lower frequencies. This road would be classified as ISO-B for low frequencies.

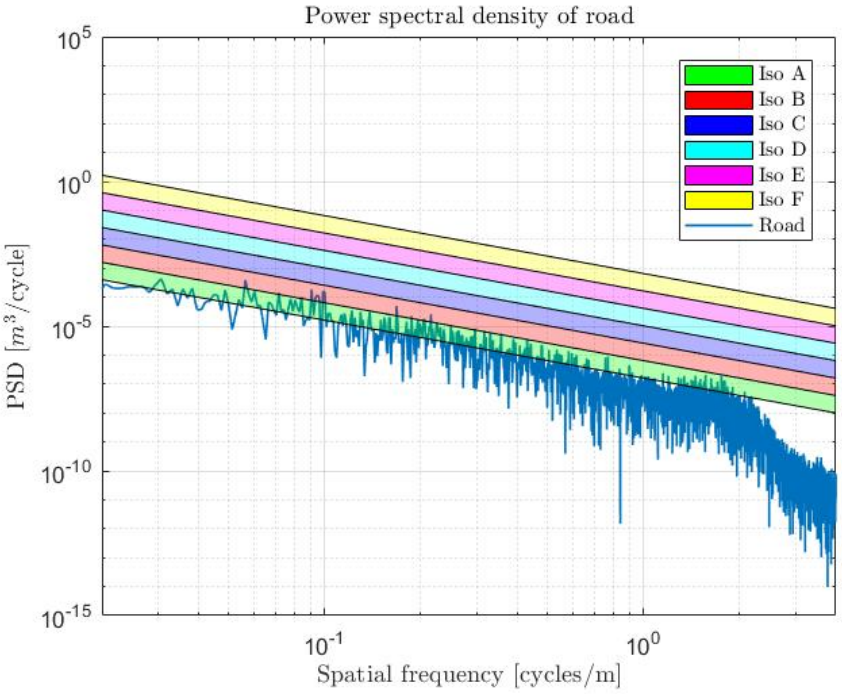

Figure 5.10: *PSD plot of road C for right side of vehicle with ISO classification*

In table 5.3 the comfort and road holding values for the different test cases, while driven on road C, can be seen. The respective PSD plots for body acceleration and tire deflection can be seen in appendix C.

Table 5.3: *Comfort and road holding values for road C*

	RMS $\ddot{z}_s$ [m/s^2]			Peak jerk [m/s^3]	RMS z_{def_t} [m]
	1-4Hz	4-8Hz	8-20Hz	-	0.5-30Hz
Force gain = 0.5	0.212	0.09	0.093	119	0.000641
Force gain = 0.75	0.205	0.096	0.096	138	0.000643
Force gain = 1	0.201	0.102	0.099	140	0.000648
Rate limit = 0.001	0.243	0.082	0.088	104	0.000667
Rate limit = 0.5	0.199	0.104	0.1	168	0.000648
Rate limit = 1.6	0.199	0.104	0.1	169	0.000648
Spring gain = 0.75	0.167	0.096	0.098	157	0.000597

In figure 5.11 the trade-off between road holding and comfort can be seen for the different test cases. The lowered spring rate results in both improved comfort

and road holding, similar to previous cases. Interesting to note is how both road holding and comfort is improved with lowered force gain. The lowered rate limit lead to improved comfort with an arguably small trade-off for road holding.

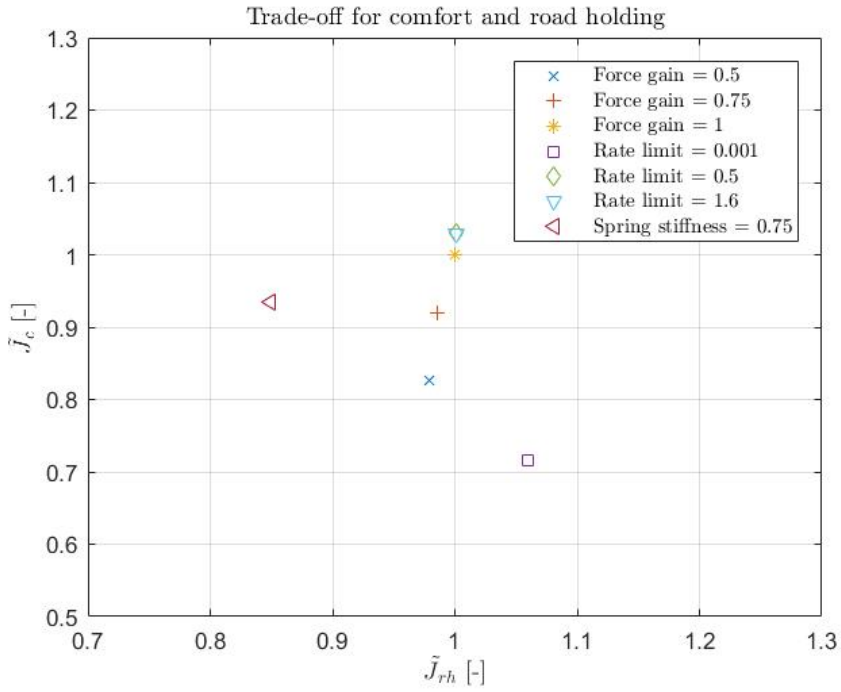

Figure 5.11: *Trade-off between road holding and comfort with force gain set to 1 as reference*

The worst comfort was achieved with rate limit set to 0.5. Compared with Janeway's comfort criterion, shown in figure 5.12, it can be seen that the comfort parameters are still well within the limits.

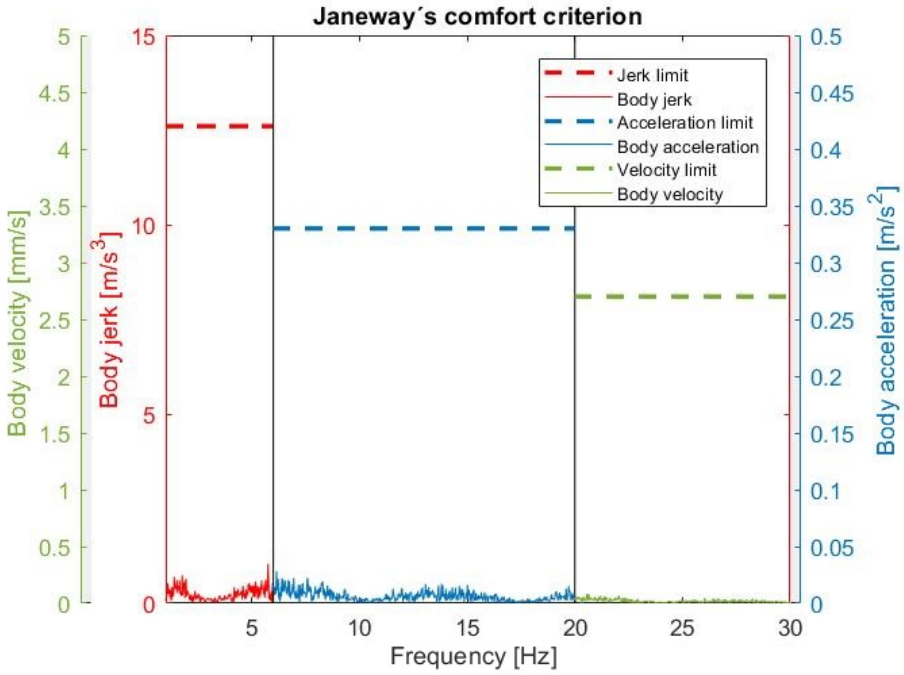

Figure 5.12: *Janeway's comfort criterion for rate limit set to 0.5*

5.2.4 Road D

Road D was created in order to simulate some typical primary and secondary ride conditions. Both driving conditions were modeled as combinations of sine waves with various amplitude at various frequencies, where the primary ride part of the road mainly consists of low frequency waves and the secondary ride mainly consists of high frequency waves. The road profile can be seen in figure 5.13, where the primary ride appears during the initial 15 seconds of the road and the secondary ride during the latter part. The PSD plot for the primary and secondary ride parts of the road can be seen in figure 5.14. The shape of both parts of the road is straight.

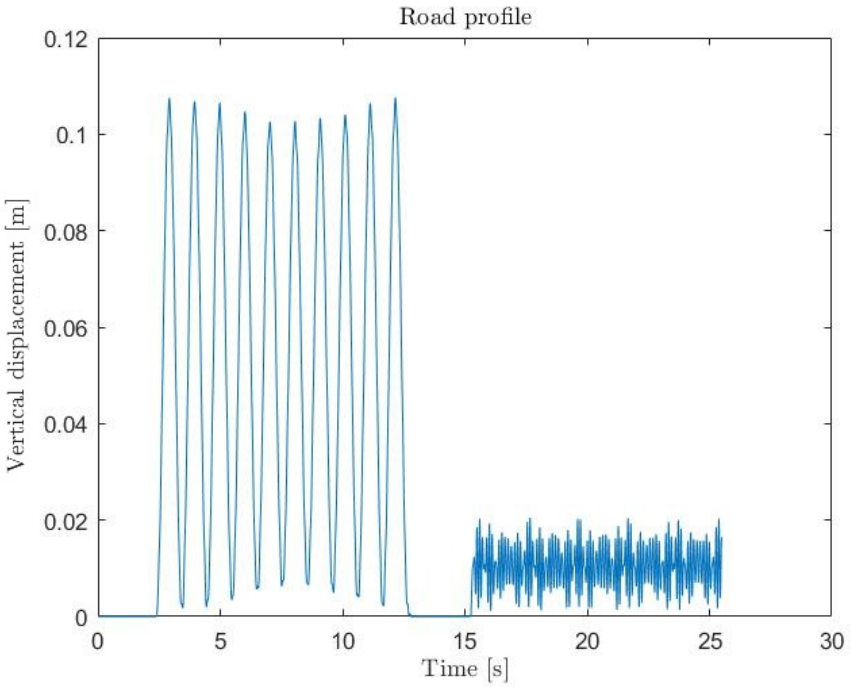

Figure 5.13: *Road profile of road D*

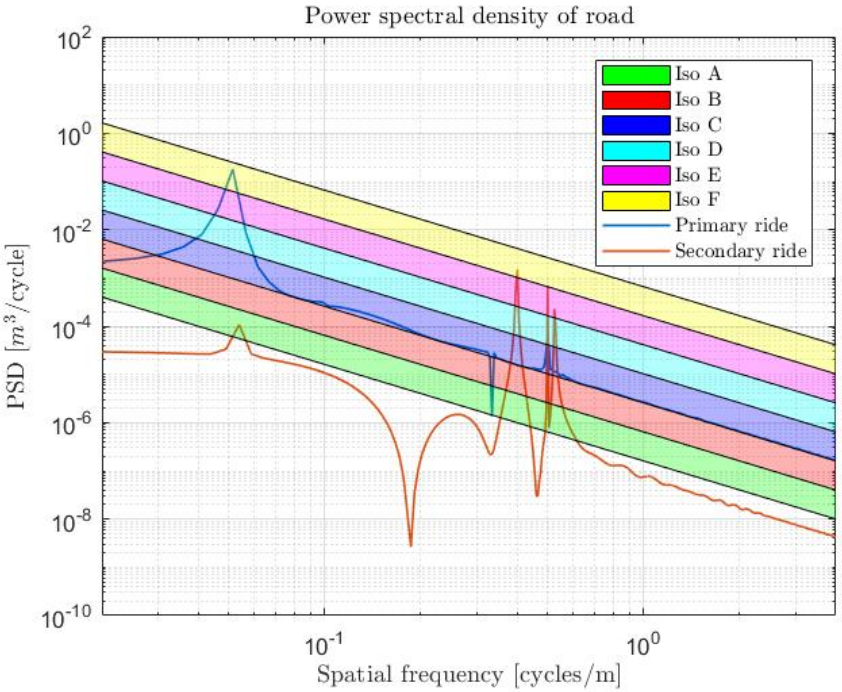

Figure 5.14: *PSD plot of primary and secondary ride parts of road D with ISO classification*

In table 5.4 and 5.5, the road holding and comfort values can be seen. The respective plots for body acceleration over time and tire deflection over time can be seen in appendix D. For the primary ride part of the road it can be seen that both road holding and comfort are worsened with lowered force gains and lowered rate limit. The lowered spring stiffness shows improved road holding but decreased comfort.

For the secondary ride part of the road, opposite results are achieved where both road holding and comfort are improved with the lowered force gains and lowered rate limit. The lowered spring gain leads to an improvement in ride comfort with a trade-off for decreased road holding.

Table 5.4: *Comfort and road holding values for the primary ride part of road D*

	Primary ride		
	RMS $\ddot{z}_s$ [m/s^2]	RMS z_{def_t} [m]	Peak jerk [m/s^3]
Force gain = 0.5	2.113	0.00348	90
Force gain = 0.75	2.086	0.00334	100
Force gain = 1	2.078	0.00331	101
Rate limit = 0.001	2.167	0.00385	73
Rate limit = 0.5	2.077	0.00331	99
Rate limit = 1.6	2.077	0.00331	100
Spring gain = 0.75	2.265	0.00303	133

Table 5.5: *Comfort and road holding values for the secondary ride part of road D*

	Secondary ride		
	RMS $\ddot{z}_s$ [m/s^2]	RMS z_{def_t} [m]	Peak jerk [m/s^3]
Force gain = 0.5	0.609	0.00138	739
Force gain = 0.75	0.612	0.0014	744
Force gain = 1	0.617	0.00144	778
Rate limit = 0.001	0.611	0.00137	744
Rate limit = 0.5	0.617	0.00146	787
Rate limit = 1.6	0.617	0.00146	787
Spring gain = 0.75	0.59	0.00158	795

In figure 5.15 and 5.16 a visualization of the previously discussed results can be seen. The performance index for ride comfort and road holding was calculated as shown in equation 2.9 and 2.10, with the only difference being that the comfort index was calculated for frequencies in the range of 0.5-20Hz. The primary ride part of road D shows the best results for the cases force gain set to 1 and rate limits set to 0.5 and 1.6. The lowered spring gain result in decreased comfort but improvement in road holding.

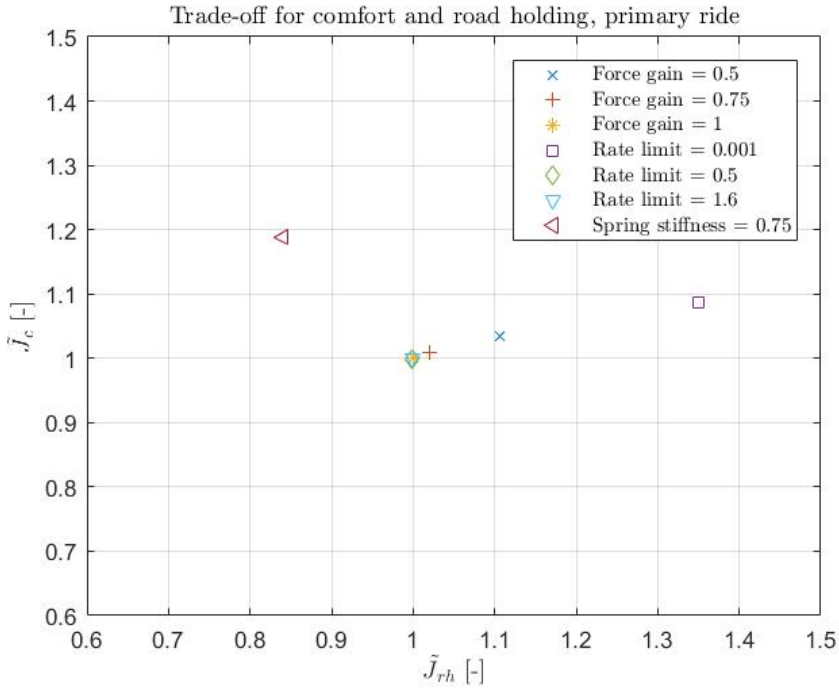

Figure 5.15: *Trade-off between road holding and comfort with force gain set to 1 as reference for the primary ride part of road D*

For the secondary part of road D all control methods that lead to lowered damping show improved results in terms of both comfort and road holding. It can also be seen that the lowered spring stiffness leads to improved road holding but decreased comfort for the general primary ride part of the road while improved comfort and decreased road holding is seen for the secondary ride part of the road.

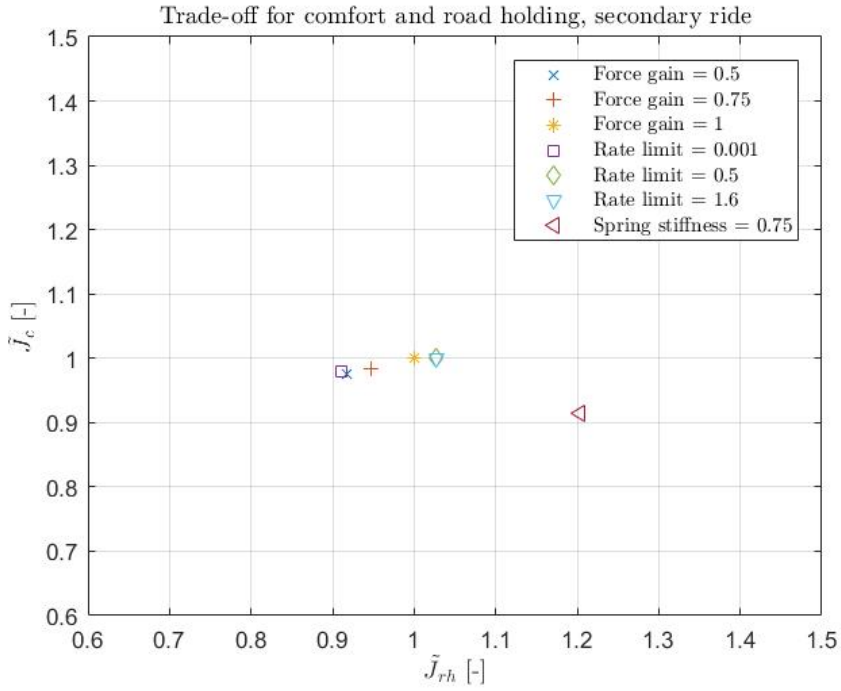

Figure 5.16: *Trade-off between road holding and comfort with force gain set to 1 as reference for the secondary ride part of road D*

5.3 Result comparison

An increase in rate limit resulted in a loss of comfort for all test cases. Although a slight improvement in road holding was seen on road B, the improvement can be viewed as non-recongnizable in real world driving. If the damping were to be controlled with this method the rate limits should thus not be increased above 0.05A/ms.

The lowered force gains resulted in similar behaviour as the lowered rate limits. The lowered rate limit did yield a larger trade-off between road holding and comfort for all roads which comes down to the rate limit being set at 0.001A/ms being an objectively more aggresive tuning value compared to e.g. force gain set to 0.5 or 0.75.

Comparing road B to road A, similar behaviour can be seen as the cases with lowered force gain and lowered rate limit lead to improved comfort. The difference for road B, compared to road A, is that the trade-off is larger and a larger amount of road holding has to be sacrificed in order to achieve improved comfort.

A correlation can be seen for the trade-offs and frequency components for the

various roads. Road B and C are very similar in terms of high frequency amplitude, but presents a different classification for low frequencies which causes the trade-offs for road B, seen in figure 5.7, and road C, seen in figure 5.11, to present different results. By comparing the test case with rate limit set at 0.001A/ms for both roads it can be seen that the trade-off is significantly higher for road B than road C. The lowered rate limit can provide an overall higher comfort improvement on road B, but then an almost as high amount of road holding will need to be sacrificed. On road C a large comfort improvement can be seen with the rate limit set to 0.001 with a small trade-off for road holding.

The peak jerk showed a clear correlation between the amplitude of the disturbances at high frequencies, where a larger amplitude led to significantly increased peak jerk values, shown in section 5.2.1, compared to when e.g. road C, shown in section 5.2.3. which further showcases the importance of proper damper control for high frequencies. For the rough road, presented in section 5.2.1, a correlation between peak jerk values and amount of damping could not be seen, which was more apparent for the low frequency roads, presented in section 5.2.2 and 5.2.3. The reasoning for this could possibly be that the CCD model is modeled with a bandwidth and that the highest peak jerk values were for frequencies outside the damper working region. For the secondary ride part of road D, seen in section 5.2.4, the peak jerk is lowered with a lowered amount of damping. In order to properly evaluate the validity of these results, real world tests would have to be made.

For the roads with high amplitudes at high frequencies, road A and the secondary ride part of road D, it could be seen that the lowered spring stiffness resulted in improved comfort and loss of road holding ability. While for roads with a small amount of high frequency content, both improvements in road holding and comfort could be seen with a lowered spring stiffness. Although the primary ride part of road D, seen in figure 5.15, showed a loss of comfort for mainly low frequency disturbances, this would come down to the fact that the high frequency disturbances were more or less non existent. For a similar road in real world driving, the high frequency content would be more recognizable and thus allow for the softer spring to lower the transmissibility of the disturbances.

6
Discussion

Roads that are classified according to ISO 8608 are generally done so with respect to the highest amplitude of the road. The problem with this sort of classification is that is does not take the amplitude of the other frequencies into consideration. The results in this thesis have shown that it is important to have a general idea of the entire frequency spectra in order to properly be able to weigh the trade-off between comfort and road holding.

When the comfort objective was analyzed it was mainly done so over the frequencies 4Hz to 20Hz. The reasoning behind this is that the body accelerations that are felt for frequencies lower than 4Hz are connected to the primary ride. If vehicle were to be driven on a road with high amplitude disturbances at low frequencies, the driver would achieve better comfort if they were to slow down rather than tune the damper differently.

The test cycles in this thesis were carried out on a variety of roads with a set load and speed. Since it's known that low speeds improve primary ride behaviour and high speeds improve secondary ride behaviour, analysis of the results can be carried out appropriately without having to make separate tests at different speeds. Similar things can be said for varying the vehicle load. Instead of conducting tests for every possible load, one test for a low load and one test for a high load would be sufficient as the results for the loads in between can be estimated through the other results.

During the earlier stages of this thesis there were plans of carrying out real world tests in order to validate the results in a real vehicle. Due to the covid-19 pandemic, these tests unfortunately had to be cancelled.

In terms of tests for different roads, it is important to use a wide variety of pro-

files, where a good mix of low and high frequency content is present. As seen in the results can the trade-off for comfort and road holding show different results depending on the profile of the road.

The varying stiffness of the air suspension was analyzed through variations in the spring stiffness of the passive spring. As mentioned in section 2.3.3, the passive spring does not take the nonlinearity of the air suspension into consideration which would appear during real world driving.

As discussed in section 2.3.3, the lower spring stiffness provides both improved comfort and road holding for most frequencies. A small amount of road holding is usually lost for high frequencies and a small amount of comfort is usually lost for low frequencies. Thus, for the cases where performance in either of these areas were lost, i.e. road D shown in section 5.2.4, it can be seen that the road disturbances were dominant on both areas in which performance was lost. Road D was also not an entirely realistic road since it was modeled manually. It can thus be concluded that a lowered spring stiffness gives better road holding and comfort for most roads.

6.1 Conclusion

i. **What strategy can be defined to weigh the damping and stiffness suspension parameters in order to improve handling and comfort for different road profile classifications?** Force gain control and rate limit control are both valid options in order to vary the vehicle damping. The rate limit should however not exceed 0.05A/ms as this will not provide any improvements in terms of both road holding and comfort.

   For general primary ride conditions a stiff damping is preferred and for general secondary ride conditions a low damping is preferred for optimal road holding and comfort.

   When the low frequency disturbances are small and high frequency disturbances has an ISO-B class or higher, the trade-off going to be small which provides the possibility of improving comfort for little to no loss of road holding. If the low frequency disturbances are significantly small, i.e. ISO-B class or lower, the low damping will also lead to improved road holding.

   As the low frequency disturbances increases in amplitude, increases the trade-off. Thus should the amount of damping be adjusted in terms of preferrability. For improved road holding, a stiff damping would be preferred and for improved comfort, a soft damping would be preferred.

   For pure primary ride conditions, a soft spring leads to improved road holding with a trade-off for comfort while for pure secondary ride conditions, a reversed trade-off can be seen. Since these conditions are very rare and general road contain a mix of primary and secondary ride, the recommendation is to always use the soft spring since this will improve both road holding and

comfort when the road is not perfectly smooth.

ii. **What performance criteria in terms of limits over different frequencies can be used to define good ride comfort and road holding?** In terms of comfort and an analysis standpoint is the ISO 2631 standard very useful since different limits are used for various lengths of exposure. Some roads will only be driven for a limited amount of time which would provide the ability to tune the dampers towards a more road holding oriented approach.

Janeway's comfort criterion was used for comfort validation in this thesis. The criterion consists of limits for peak jerk, peak acceleration and peak velocity of the body for the frequency spectras 1-6Hz, 6-20Hz and 20-30Hz. The limit for peak jerk is $12.6 m/s^3$, the limit for peak acceleration is $0.33 m/s^2$ and the limit for peak velocity is $2.7 mm/s$. It is an easy to use criterion but does not take exposure time into consideration.

In terms of road holding has no concrete critera been found. The main goal in order to improve the road holding is to reduce the distance between the wheel and the road.

iii. **What benchmarks for suspension systems can be used that are representative for different degrees of model complexity and real-world driving?** As long as the tests are carried out with identical vehicle parameters, i.e. speed, load, tire etc., the results can then be analyzed for when these parameters differ without having to conduct tests for all possible scenarios.

In terms of roads is it important to use a wide variety of roads with a mix between low and high frequency content as the trade-off can appear very different for different roads.

6.1.1 Future scope

The future scope should consist of real world tests in order to properly evaulate the damper tuning when the objective isn't clear, whether road holding or comfort should be prioritized.

Tests with on-board ISO classification of the road would be interesting to conduct since this would open for the possibility of various damper tuning whether the primary or secondary ride is dominant for a certain road.

Conduct tests for cases for a larger deadband, i.e. a lowered damper force for a larger part of the damper working region.

Conduct tests with an air-suspension model in order to capture the

Bibliography

[1] Rosheila Darus and Sam Md. Yahaya. Modeling and control active suspension system for a full car model. *2009 5th International Colloquium on Signal Processing Its Applications*, pages 13–18, 03 2009. doi: 10.1109/CSPA.2009.5069178.

[2] Bengt Jacobson et al. *Vehicle Dynamics Compendium for Course MMF062*. 2015.

[3] Omid Ghasemalizadeh, Saied Taheri, Amandeep Singh, and Jill Goryca. Semi-active suspension control using modern methodology: Comprehensive comparison study. 08 2014. doi: 10.13140/2.1.3319.0083.

[4] Emanuele Guglielmino, Tudor Sireteanu, Charles W. Stammers, Gheorghe Ghita, and Marius Giuclea. *Semi-active suspension control*. Springer., first edition, 2008.

[5] Anton Gustafsson and Alexander Sjögren. Neural network controller for semi-active suspension systems with road preview. 05 2019. URL `https://odr.chalmers.se/bitstream/20.500.12380/257298/1/257298.pdf`.

[6] M. W. Holtz, , and J. L. van Niekerk. Modelling and design of a novel air-spring for a suspension seat. *Journal of Sound and Vibration*, 329(21):4354 – 4366, 2010. doi: https://doi.org/10.1016/j.jsv.2010.04.017. URL `http://www.sciencedirect.com/science/article/pii/S0022460X10002695`.

[7] R.N Janeway. Human vibration tolerance criteria and applications to ride evaluation. 02 1975. doi: 10.4271/750166.

[8] D. Karnopp, M. Crosby, and R. Harwood. Vibration control using semi-active force generators. *Journal of Engineering for Industry*, 1974. doi: 96(2):619-626.

[9] Grzegorz Ślaski and Michal Maciejewski. Skyhook and fuzzy logic controller

of a semi active vehicle suspension. *Prace Naukowe Politechniki Warszawskiej - Transport*, 78:97–111, 01 2011.

[10] Olof Lindgärde. Kalman filtering in semi-active suspension control. 07 2002. doi: 10.3182/20020721-6-ES-1901.01541.

[11] Y. Liu, T.P. Waters, and M.J. Brennan. A comparison of semi-active damping control strategies for vibration isolation of harmonic disturbances. *Journal of Sound and Vibration*, 280(1):21 – 39, 2005. URL http://www.sciencedirect.com/science/article/pii/S0022460X04000252.

[12] Sachin Madhusudhana. Road profile estimation and classification. 08 2019. URL https://odr.chalmers.se/bitstream/20.500.12380/300324/1/Madhusudhana_2019.pdf.

[13] D. Sanunier, Olivier Sename, and Luc Dugard. Comparison of skyhook and h_∞ control applied on a quarter-car suspension model. *IFAC Proceedings Volumes*, 34:107–112, 03 2001. doi: 10.1016/S1474-6670(17)34385-9.

[14] S. Savaresi, E. Silani, and S. Bittanti. Semi-active suspensions: an optimal control strategy for a quarter-car model. pages 572–577, Salemo, Italy, 2004.

[15] S. Savaresi, E. Siciliani, and S. Bittanti. Acceleration driven damper (add): an optimal control algorithm for comfort oriented semi-active suspensions. *ASME Transactions: Journal of Dynamic Systems, Measurement and Control*, 2005. doi: 127(2):218-229.

[16] Sergio Savaresi and Cristiano Spelta. Mixed sky-hook and add: Approaching the filtering limits of a semi-active suspension. *ASME Transactions: Journal of Dynamic Systems, Measurement and Control*, 2007. doi: 129(4): 382-392.

[17] Sergio Savaresi, Charles Poussot-Vassal, Cristiano Spelta, Olivier Sename, and Luc Dugard. Semi-active suspension control design for vehicles. *Semi-Active Suspension Control Design for Vehicles*, 08 2010. doi: 10.1016/C2009-0-63839-3.

[18] Stamat Stamatov, Mohan Krishnan, and Sandra Yost. Low jerk predictive force modulation for semi-active suspension control. 04 2008. doi: 10.4271/2008-01-0904.

Appendix

A

Road A

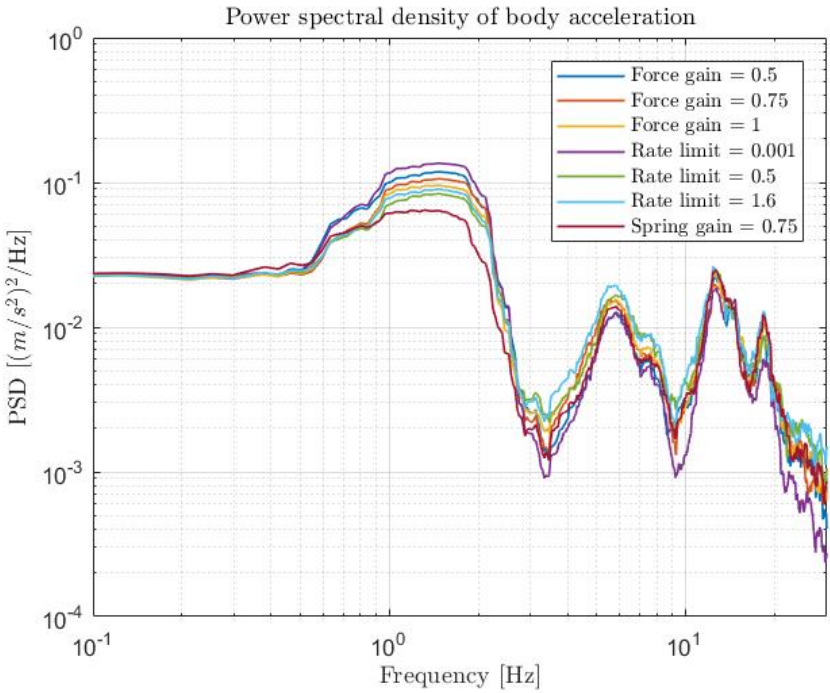

Figure A.1: *PSD plot of body acceleration*

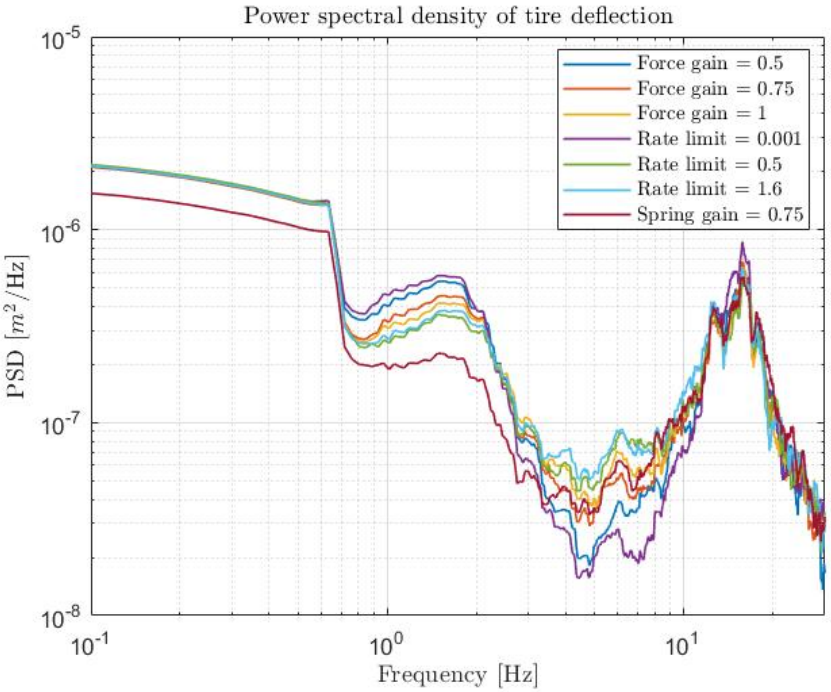

Figure A.2: *PSD plot of tire deflection for the front right wheel*

B

Road B

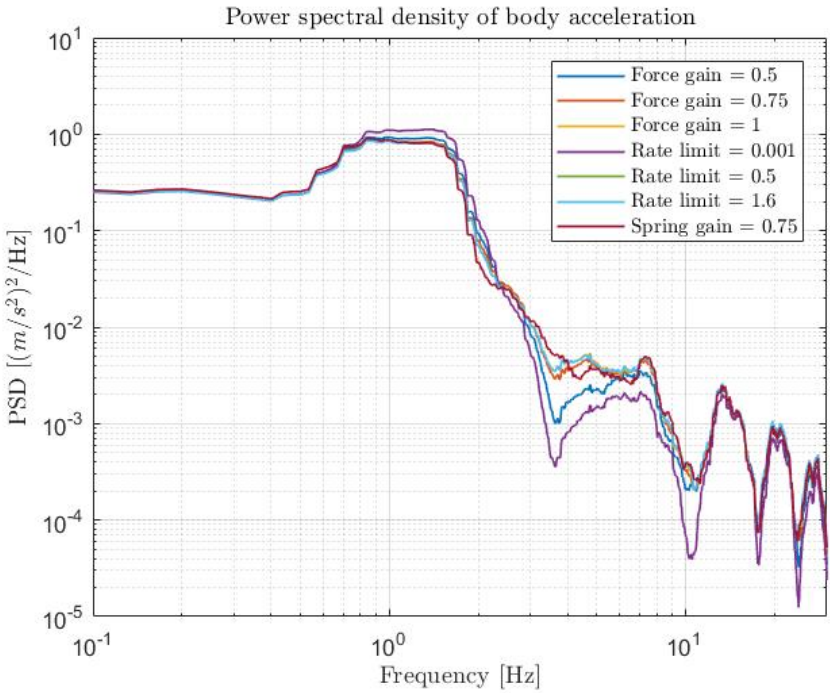

Figure B.1: *PSD plot of body acceleration*

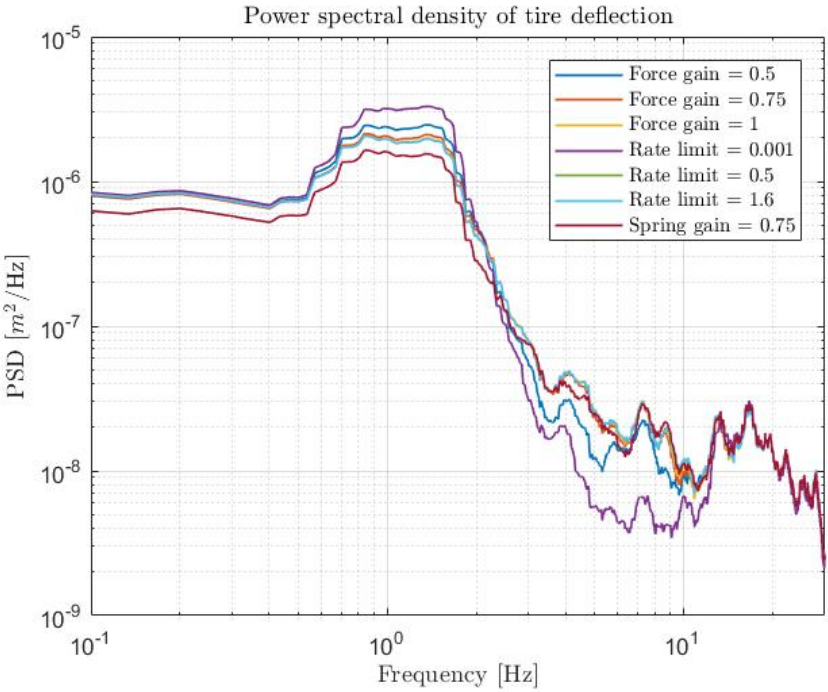

Figure B.2: *PSD plot of tire deflection for the front right wheel*

C

Road C

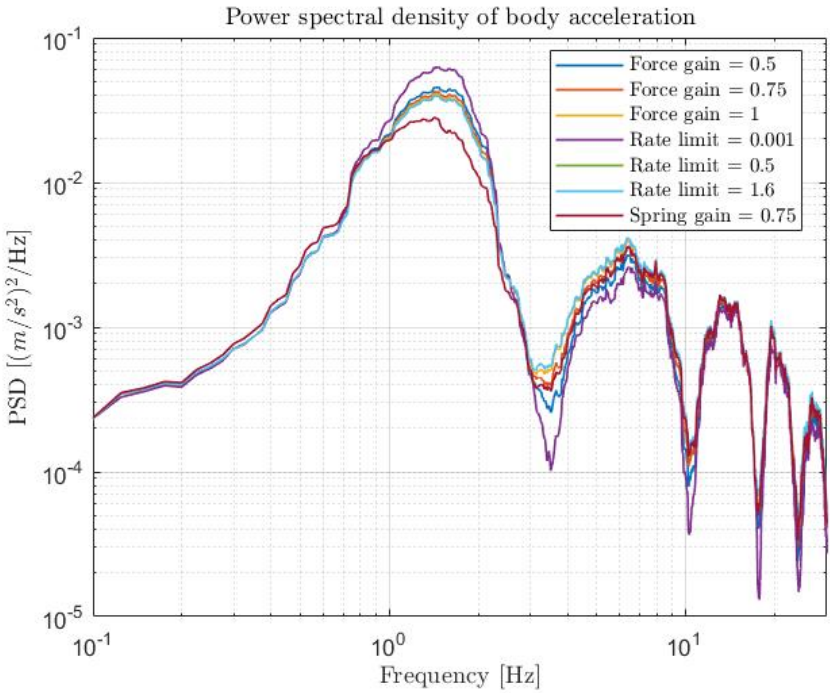

Figure C.1: *PSD plot of body acceleration*

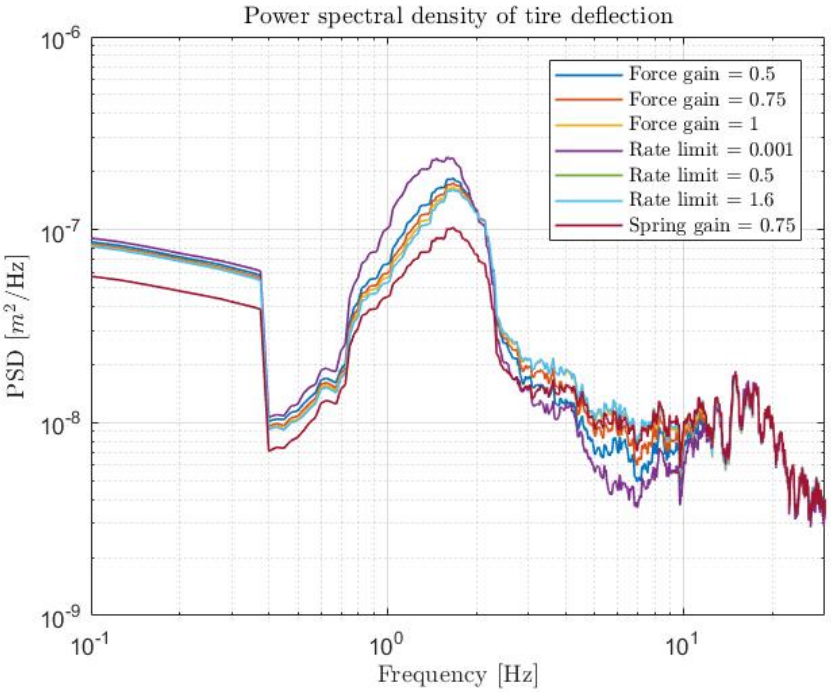

Figure C.2: *PSD plot of tire deflection for the front right wheel*

D

Road D

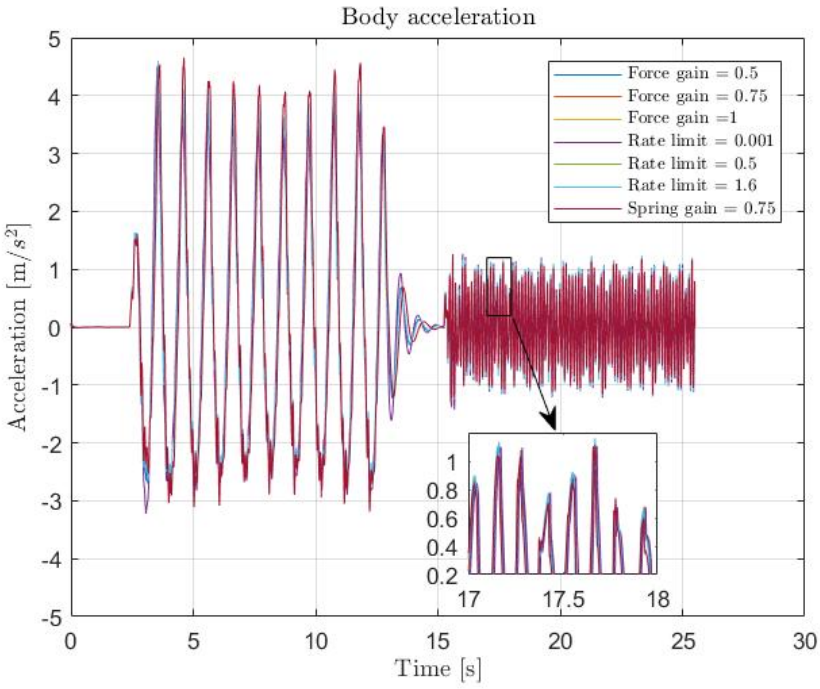

Figure D.1: *Plot of body acceleration over time*

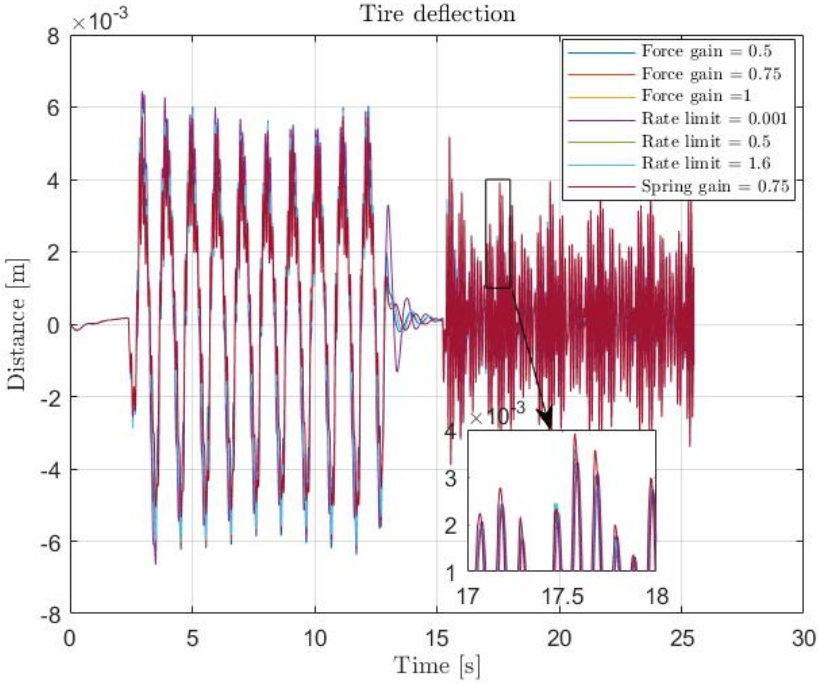

Figure D.2: *Plot of tire deflection over time*